Distribution Agreement

In presenting this thesis or dissertation as a partial fulfillment of the requirements for an advanced degree from Emory University, I hereby grant to Emory University and its agents the non-exclusive license to archive, make accessible, and display my thesis or dissertation in whole or in part in all forms of media, now or hereafter known, including display on the world wide web. I understand that I may select some access restrictions as part of the online submission of this thesis or dissertation. I retain all ownership rights to the copyright of the thesis or dissertation. I also retain the right to use in future works (such as articles or books) all or part of this thesis or dissertation.

Signature:

_____ _____

Zhuyun Mao Date

Epigenetic Associations of Circulating Interleukin 6 among People with HIV

By

Zhuyun Mao
Master of Public Health

Department of Epidemiology

_____

Yan Sun, Ph.D
Committee Chair

Epigenetic Associations of Circulating Interleukin 6 among People with HIV

By

Zhuyun Mao

Bachelor of Science
University of Minnesota, Twin Cities
2019

Thesis Committee Chair: Yan Sun, Ph.D

An abstract of
A thesis submitted to the Faculty of the
Rollins School of Public Health of Emory University
in partial fulfillment of the requirements for the degree of
Master of Public Health
in Department or Epidemiology
2021

Abstract

Epigenetic Associations of Circulating Interleukin 6 among People with HIV
By Zhuyun Mao

Background
Interleukin-6 (IL-6), the proinflammatory cytokine, is a key signal transducer in response to the viral infection. Elevated plasma levels of IL-6 were associated with mortality in people with HIV (PWH). Inflammation and immune responses could be regulated by epigenetic modifications. An Epigenome-Wide Association study (EWAS) was conducted to investigate the epigenetic association with-IL-6 among PWH.

Method
Peripheral blood samples from the Veterans Aging Cohort Study (VACS) participants were investigated for epigenome-wide DNA methylation (DNAm) levels using the Illumina Infinium Methylation 450K (n=512) and EPIC BeadChip (n=490). An epigenome-wide discovery, replication and meta-analysis were performed to identify the significant epigenetic associations with IL-6 using multiple regression models adjusted for covariates and batch effects.

Results
In the meta-analysis of 1,002 male veterans with HIV, 111 DNAm sites were significantly associated with IL-6 after correction for multiple testing. The identified IL-6-associated DNAm site were highly concordant between the 450K and EPIC sub-cohorts. The top IL-6--associated DNAm sites mapped to genes including *VMP1*, *IFITM1*, *STAT1*, and *MX1*, all related to innate immune responses and antiviral response.

Discussion
The key findings of the principal genes and the pathways epigenetically related to the IL-6 levels could help understand the chronic inflammation mechanisms of HIV infection. The robust findings of IL-6-assocaited DNAm sites may uncover potential-therapeutic targets related to key pathways influencing the immune recovery and chronic disease outcomes among PWH.

Conclusion
This EWAS summarized *VMP1*, *IFITM1*, *STAT1*, *MX1* and *OSA1* genes related to IL-6 methylation among PWH. Those DNAm sites are helpful to further investigate the pathogenesis of inflammation and can imply as a necessary accompaniment to study the chronic diseases and survival status of HIV infection.

Epigenetic Associations of Circulating Interleukin 6 among People with HIV

By

Zhuyun Mao

Bachelor of Science
University of Minnesota, Twin Cities
2019

Thesis Committee Chair: Yan Sun, Ph.D

A thesis submitted to the Faculty of the
Rollins School of Public Health of Emory University
in partial fulfillment of the requirements for the degree of
Master of Public Health
in Department or Epidemiology
2021

Acknowledgments

During this COVID pandemic, although there were multiple challenges and difficulties during this thesis work; I would like to express my sincere gratitude to many people who have helped through this time. First and foremost, I am extremely grateful to my thesis advisor, Dr. Yan Sun for his invaluable advice, continuous support, and patience during my thesis work. His immense knowledge and plentiful experience have encouraged me in all the time of my academic research and daily life. I would also like to thank Zeyuan Wang and Dr. Hui Qui for their analytical and computational support for my thesis. I would like to thank all the members in the Dr. Yan Sun's team providing me with thoughtful suggestions for my thesis research. Also, I would like to thank my boyfriend, Jiahui Jiang, for his companion and support through this difficult time during COVID pandemic. Finally, I would like to express my gratitude to my parents although we haven't met for almost two years. I really miss them and without their tremendous understanding and encouragement in the past few years, it would be impossible for me to complete my study in the US.

Table of Contents

Introduction

Human immunodeficiency virus (HIV) infection causes series of chronic diseases and complications and is a major public health concern (1). About 38 million people were infected globally with HIV in 2019 (2). Around 40,000 new cases of HIV infection were reported in the United States in 2019 (3). Globally, 95% of people with HIV (PWH) live in developing countries who experience low income, social inequalities, and insufficient healthcare infrastructure (4). No cure for HIV infection exists at the current stage. Uncontrolled HIV infection could compromise the human immune system leading to acquired immunodeficiency syndrome (AIDS), which was the most severe end stage of HIV infection, the life-threatening health impact for PWH (5).

Antiretroviral treatments (ART) have demonstrated high efficacy in suppressing HIV replication (6) to keep PWH at the stage of HIV chronic infection (7). With successful viral load control by ART, HIV infection hardly causes AIDS and direct fatality; however, other chronic disease complications for PWH still pose a substantial public health burden. HIV infection has been associated with a number of comorbidities including cardiovascular diseases, diabetes, chronic kidney diseases, cancer and hepatic diseases (e.g., chronic liver disease and Hepatitis B and C infection) (8). HIV infection may accelerate biological aging including immunosenescence to increase these chronic disease morbidities and mortality. Therefore, understanding chronic inflammation and immunological recovery of PWH may hold the key for further reducing the health burden of HIV infection.

Inflammation is crucial in the invasion of pathogens for humans (9). Chronic inflammation symptoms could play an important role in the mechanisms of comorbidities among PWH such diabetes, cardiovascular diseases (10). Several mechanisms linked to the chronic inflammation among PWH were discussed during HIV infection including the direct or indirect

pathways. $CD8^+$ T cell activation would be stimulated by the adaptive immune response during HIV infection and the increased $CD8^+$ T cells could continuously replicate the virus during HIV chronic infection (11). Another mechanism described in *Appay, V., & Sauce, D.* involves with infections by other viruses together with HIV-1 causing the depletion of $CD4^+$ T cells to favor the viral replication. The depletion of $CD4^+$ T cells would compose mucosal barriers in the gut preventing the translocation of the gut microbiota. Thus, the pathogens would be limited to the lamina propria and the mesenteric lymph nodes. Lipopolysaccharide (LPS) plasma levels would increase during HIV-1 infection to trigger the innate immune response by producing the pro-inflammatory cytokines such as TNFα, interleukin 6 (IL-6) and IL-1β (11). The immune activation and chronic inflammation among PWH would cause consequences of developing chronic diseases including chronic kidney dysfunction and diabetes due to the weakened immune systems; thus, understanding the mechanisms between the inflammation markers and the chronic inflammation among PWH could help improve the prevention and the treatment of HIV infection (12). Accelerated aging, chronic morbidities and mortality among PWH associated with multiple well-studied biomarkers including IL-6 (13).

IL-6, the proinflammatory cytokine, plays a significant role in response to the viral infection (14). Primarily, IL-6 functions as the mediator to increase Th17 cells while the level of IL-6 is increasing (15). The increase in Th17 differentiation can lead to the autoimmunity chronic inflammation (16). Simultaneously, *Hirano et al* indicated that increased IL-6 production would prohibit the apoptosis of cells by inhibiting the CD8 helper T cells. Many studies throughout the years have shown the role of elevated plasma IL-6 levels in HIV infection, morbidities and mortality among PWH (17) and ART treatment can activate the production of IL-6 (18). Previous studies have investigated the association between the concentration of viral

load of HIV and the level of circulating IL-6 and other inflammatory cytokines (19). Many pro-inflammatory cytokines such as interleukin 1β, IL-6, tumor necrosis factors (TNF-α) or interleukin 8 were detected higher in the blood serum samples in HIV infected patients compared to healthy individuals in the previous study (20,21). Higher levels of plasma IL-6 levels are related to HIV replication and low nadir CD4 cell counts (19). A study demonstrated that elevated levels of IL-6 representing the activated inflammation was associated with multiple clinical endpoints of HIV-associated morbidities such as the cardiovascular diseases among HIV-positive persons (22). The association between the IL-6 concentration and HIV replication or viral load among PWH has been confirmed and nongenetic factors were discovered linked to HIV infection including alcohol use, smoking, obesity and education level (19,23). Genetic changes in gene expression excluding the mutation or sequence change of the genome are considered as epigenetic modification which includes the chemical alteration on DNA sequence (24).

Epigenetic modification is mostly studied on the DNA methylation (DNAm) in the population level and DNAm has been associated with HIV infection and viremia (25). The host genome in PWH could be integrated by epigenetic mechanisms and epigenetic changes can reprogram the host genes in viral latency (26). Several Epigenome-wide Association Studies (EWAS) have discovered and replicated the DNAm sites associated with HIV infection as well as the related diseases among PWH (25). A recent study has identified 15 novel epigenetic associations with estimated glomerular filtration rate among PWH and suggested the potential epigenetic mechanisms of HIV-related chronic kidney diseases (CKD) risks (27). Some EWAS related to inflammatory biomarkers such as C-reactive proteins (CRP), and interleukins were

also conducted. However, the results of the DNAm sites were not consistent across the studies (28,29) and may not be able to represent the epigenetic associations among PWH.

Although IL-6 is a key cytokine in regulating inflammatory pathways, only a few EWAS have investigated the DNAm sites associated with IL-6. A recent study has discovered a few hypermethylation DNA sites associated with IL-6 plasma level among community-dwelling adults (30). Another study in a community-based setting showed elevated IL-6 serum levels among lifetime depression patients and IL-6 methylation was discovered as an inverse correlation with circulating IL-6 (31). The study among women with breast cancers showed the decreased methylation 5'-C-phosphate-G-3' (CpG) sites and lower methylation at each identified CpG site was associated with increased IL-6 plasma levels after the chemotherapy treatment (32). Despite of the associations of circulating IL-6 and the DNAm sites of IL-6 among other diseased populations, no EWAS indicates the IL-6 DNAm associations among PWH. Although the relationship between IL-6 and various aspects of HIV infection was proved to be associated, no current EWAS is clear about the genetic and environmental factors associated with IL-6 among PWH. Thus, in this study, EWAS approach was performed to identify the IL-6 DNA methylation sites related to the HIV infection. Significant CpG sites were identified by meta-analysis and replication analysis. We also examined the previously identified IL6-associated DNAm sites in other diseases and discovered some novel CpG sites with IL6 DNAm among PWH.

Methods

Study sample

A prospective, observational cohort study of veterans including HIV positive and negative patients, the Veterans Aging Cohort Study (VACS), in care at the Department of Veterans Affairs medical centers across the United States, was used to determine the phenotypic and epigenetic data matching on sex, race/ethnicity and age (25). VACS dataset was approved by the institutional research board committee at the Connecticut veteran healthcare system. HIV positive and negative patients have been seen in eight different veteran medical centers and general medical clinics since 1997 with electronic medical records collected for each patient. Within the clinical records, total white blood cell counts and $CD4^+$ T cell counts were collected at the time of peripheral blood sample collection (25).

Interleukin 6 (IL-6) was measured in blood serum using ELISA kit. The normal range of IL-6 is between 0 to 16.4 pg/mL (33). Covariates including age, race, BMI, hepatitis B virus (HBV) infection status, hepatitis C virus (HCV) infection status, smoking status (current smoking vs noncurrent smoking), diabetes status, alcohol usage (hazardous vs non-hazardous use), HIV RNA viral load (threshold of 75 copies per milliliter), ART use were described in Table 1. The study was approved by the Veteran's Administration Research and Development Committee and the Institutional Review Board of Atlanta Veteran's Administration.

DNA Methylation data processing and quality control

The epigenome-wide DNA methylation was measured from previous studies using the Illumina Infinium HumanMethylation450 (450K) BeadChip and the Infinium MethylationEPIC (EPIC) BeadChip, respectively (34,35). DNA methylation samples in these two chips were measured from the peripheral blood monocellular cells (25). Quality control was performed for data normalization and batch correction using subset-quantile within array normalization (36).

To help correct the methylation signals and to generate adjusted β-values, both 450K and EPIC subset were processed by a quantile normalization approach in the R package "*minfi"* (27). After the quality control, 412,583 autosomal chromosome sites from 450K array subset (n=512) and 846,604 autosomal chromosome sites from EPIC array subset (n=490) remained for the epigenetic association analysis.

Statistical analysis

450K and EPIC arrays were analyzed separately for IL-6 EWAS. The linear mixed regression model was conducted for the effect of methylation status at individual CpG sites on IL-6 with each array. In addition to the phenotypes included in Table 1, the heterogeneity of cell type proportions in blood and other tissues is a well-stablished confounder in epigenetic association studies and was adjusted for in this study using calculated cell type proportions (CD4+ T cells, CD8+ T cells, NK cells, B cells, monocytes, and granulocytes) in the blood (37). Serum level of IL-6 was not normally distributed with extreme outliers of 206 pg/mL; thus, the IL-6 levels were normalized using boxplot to remove the outliers which extend more than three box-lengths (38). 49 and 41 observations were excluded from the 450K and EPIC chip subsets, respectively. After the removal of the IL-6 outliers, the total sample size of this EWAS was 512 in 450K array and 490 in EPIC array. IL-6 levels in the unit of pg/mL were analyzed in the association analysis without transformation.

The linear mixed model was implemented using the R *nlme* package to identify IL-6 associated DNA methylation sites controlling for covariates listed below.

$$Model: \quad DNAm \sim IL-6 + Age + BMI + Diabetes + alcohol\ use + smoking\ status + viral\ load\ level + HCV\ status + HBV\ status + Antiretroviral\ therapies + \text{calculated cell} + \text{type proportions}$$

The DNAm levels of each site was modeled as a dependent variable with random effect for each chip. The random intercept was included for each chip to correct the potential correlation of sample processing. The Bonferroni correction p-value was calculated based on the number of CpG sites analyzed in this EWAS to adjust for multiple testing.

Replication and Meta-Analysis

For DNAm sites measured in both the 450K and EPIC subsets, we examined the consistency of the associations with IL-6 by bidirectional replication of the significant associations identified in each subset (FDR q-value <0.05). We compared the directionality of identified associations as well as the statistical significance threshold after correction of multiple testing. Inverse-variance weighted fixed-effects meta-analysis was conducted among the 356,071 DNAm sites tested in IL-6 EWAS of both 450K and EPIC. A Bonferroni correction p-value of 0.05 (i.e., nominal p-value of 1.4×10^{-7}) were calculated for this meta-analysis as the epigenome-wide significance threshold. The epigenome-wide significant CpG sites were reported at the threshold of p-value 1.4×10^{-7} (Bonferroni p-value <0.05) after meta-analysis among a total of 356,071 tests and the heterogeneity between two chips. The beta coefficients of the epigenome-wide significant DNAm sites from 450K and EPIC chips were compared for consistency. The overall correlation between the beta coefficients was calculated by Pearson correlation.

Pathway Enrichment Analysis

Pathway enrichment analysis was performed using the online tool DAVID Functional Annotation Bioinformatics Microarray Analysis to obtain the annotated gene information from the epigenome-wide significant DNAm sites from meta-analysis results.

Results

Demographic and clinical characteristics were summarized in Table 1 including 490 HIV-positive patients in EPIC array and 512 HIV-positive patients in 450K array. The average IL-6 serum level was 2.20 pg/mL in EPIC chip and was 2.40 pg/mL in 450K chip. 83.4% of the participants in 450K chip received ART. Similarly, 83.9% of the participants in EPIC chip received ART. All participants were males with the average age of 51.5 years old in EPIC chip and 52.1 years old in 450K chip. The average BMI in EPIC was 26.2 kg/m^2 with 80.8% African American participants and mean BMI of 25.7 kg/m^2 in 450K chip with 84.0% African American participants. Among all 490 participants in EPIC array, 76.7% were current smokers and 60.0% had the abuse alcohol use while 79.7% of the participants in 450K chip were current smokers and 41.8% had the abuse alcohol use. The phenotypic characteristics did not differ significantly between the EPIC chip and the 450K chip except HBV and cell type proportions based on the t-tests and the Chi-squared tests at the significance threshold of p-value of 0.05.

Individually EWAS in EPIC and 450K chips, there were 22 and 25 DNAm sites significantly associated with IL-6, respectively, at the threshold of Bonferroni corrected p-value less than 0.05, identified for the methylation sites in the model adjusting age, race/ethnicity, binary viral load, BMI, smoking status, alcohol use, ART use, diabetes status, HBV/HCV status and cell type proportions. Manhattan and QQ plots were created with inflation factor indicating the distribution between the expected and observed p-values for EPIC (Supplementary Figure 1) and 450K chip (Supplementary Figure 2), respectively. The most significant site in EPIC chip was identified to be cg05475649 (-0.022, p-value 5.32×10^{-10}); however, this site was not measured in 450K subset. Supplementary Table 1 summarized directionality consistency for both EPIC and 450K chip. Among EPIC array, only 11 DNAm sites were measured in 450K chip but all 11 DNAm sites showed consistency in directionality and 100% with nominal p-value less

than 0.05. Among 450K chip, 19 out 25 DNAm sites were replicable in EPIC chip and all showed consistency in directionality. Among those consistent sites, 63.2% has nominal p-values less than 0.05 significance and 21.1% were significant after multiple testing correction (Supplementary Table 1). Supplementary Table 3 summarized the information of the DNAm sites significant in EPIC chip but not measured in 450K subset.

The meta-analysis of the 450K and EPIC EWAS results identified 111 DNAm sites (Supplementary Table 2) significantly associated with IL-6 levels at the threshold of nominal p-value of 1.40×10^{-7} (Bonferroni corrected p-value < 0.05) among 1,002 PWH. These IL-6 associated DNAm sites span 9 genes on 20 autosomes (Figure 1). The overall inflation factor was 1.28 (Figure 2). Hypomethylation of cg16936953 (*VMP1*), was the most significantly associated with elevated circulating levels of IL-6 (Table 2, beta coefficient -0.0194, p-value 8.89×10^{-21}). Total of five DNAm sites in *VMP1* gene region were significantly associated with IL-6 levels (Supplementary Table 2). Both the EPIC (-0.021, 95% CI: -0.020 to -0.023) and 450K (-0.018, 95% CI: -0.020 to -0.021) chips replicated this site. *IFITM1* gene also harbored seven DNAm sites significantly associated with IL-6 levels. Two and three significant DNAm sites were located in *STAT1* gene and *MX1* gene, respectively. The beta coefficients of these 111 DNAm sites were highly correlated ($R^2 = 0.947$) between the 450K and EPIC subsets, showing very consistent associations from both microarray platforms (Figure 3). Among 111 IL-6 associated DNAm sites, hypomethylation of 88 DNAm sites (79.3%) were associated with elevated IL-6 levels indicating the demethylation was linked with increased inflammation among PWH.

The pathway enrichment analysis presented the pathways for these 81 unique genes. Table 3 summarized the top significant pathways with genes listed at the threshold of FDR q-

value lower than 0.05. The pathways included the type-1 interferon signaling pathway, interferon-gamma mediated signaling pathway, defense to the virus, antiviral defense, response to the virus, immunity, and innate immunity.

Discussion

In this EWAS of IL-6, which is an important pro-inflammatory cytokine, producing persistently higher levels in the setting of inflammation for PWH, we identified DNAm sites and genes associated with IL-6. Our EWAS has discovered statistically robust epigenetic associations and could serve as the first step to understand the role of epigenetic modifications in the pathogenesis of inflammation and potential implications for chronic diseases among PWH. This EWAS has the strength with the combined data from two different microarrays and the sample size from the combined data is relatively large. Also, it is essential to demonstrate the consistent results from both subsets regardless of the sample and technical differences. Specifically, this EWAS is focused on PWH; thus, this EWAS provided the contribution of identification of the genes related to the IL-6 methylation which had not been well studied previously.

Chronic inflammation and persistent immune activation have been a major challenge of shortened life expectancy and a higher risk of developing chronic morbidities associated with aging including cardiovascular diseases and diabetes compared to the general population with the use of ART (39). Inflammation and immune activation involve a variety of mechanisms linked with the pathogenesis of chronic HIV infection at the molecular level. One of the molecular mechanisms to mediate host genes and environmental risks is epigenetics. Since epigenetic modifications can potentially contribute to the pathological physiology among PWH, the dynamic character of the inflammatory cytokines can also cause epigenetic changes.

The top DNAm sites identified in the IL-6 EWAS were mapped to numerous genes, among which, *OAS3, STAT1, IFIT1, IFITM1, MX1 and VMP1,* are linked to inflammation and viral infection mechanisms. These genes are significantly linked to the pathways enriched from the DAVID test and *VMP1* was the top gene in the meta-analysis and was also replicated in both chips. The pathway enrichment analysis by DAVID (functional annotation clustering) (40) indicated the biological pathways of antiviral defense, innate immunity and type 1 interferon signaling as the input of 81 unique genes after meta-analysis.

STAT1, *OAS3*, *MX1*, *IFIT1*, and other six unique genes were involved in the type-1 interferon signaling pathway (FDR q-value 1.9×10^{-11}). Signal transducer and activator of transcription 1 (*STAT1*), a transcription factor which can mediate with cellular responses to interferons and other cytokines, encodes STAT1 protein (41). STAT1 can be activated by mostly the Type-1 Interferons (IFN-α and IFN-β) binding to the receptors. Notably, IL-6 can also activate STAT1 therefore leading STAT1 into the nucleus (41). Type-1 interferon and STAT1 related signaling pathways have been proved its ability of antiviral activity for the pathogenesis of HIV controlling the synthesis of multiple pro-inflammatory cytokines including IL6 (42). In our results of the pathway enrichment test, STAT1 was also involved in the IFN-γ signaling pathway (FDR q-value 1.3×10^{-5}). Moreover, previous study has identified tumor necrosis factor alpha (TNF- α) with the activation of nuclear factor kappa B (NFκB) can cause overexpression of IL6 and activate the STAT signaling pathways (43). There are multiple signal transducers and activators of transcription within the *STAT* family acting as the intracellular transcription factors mediated in immunity, apoptosis and proliferation. It is still plausible to have the abnormal expression of IL6 due to the epigenetic changes in *STAT1* gene expression along with the actively induced STAT/interferon signaling pathways thus causing a vicious cycle

among PWH. However, the evidence of the mechanisms of overexpression of IL6 and its association with epigenetic changes in *STAT1* gene still lacks. Therefore, *STAT1* could be a potential biomarker to track the expression of IL6 levels and the inflammation status among PWH. *OAS3* gene encodes the protein of 2'-5'-oligoadenylate synthase 3, an interferon-induced antiviral enzyme, which is important in inhibition of protein synthesis and viral infection resistance in innate immunity (44). Ribonuclease L (RNase L) could be activated by OAS3 therefore terminating viral replication or infection. OAS3 also was mediated in the IFN-γ signaling pathway (FDR q-value 1.3×10^{-5}) and the IL-6 increased production was induced by the increased mediated IFN-γ signaling pathway among PWH (45). *OSA3* methylation only harbored once in our EWAS meta-analysis; however, the OSA3 methylation may contribute to the IFN-γ signaling pathway against HIV infection. The Myxovirus (Influenza) Resistance 1 gene (*MX1*) is also an interferon-induced gene encoded the interferon-induced GTP-binding protein MX1 which is specifically against influenza virus infection (46). However, MX1 cannot restrict the retroviral invasion including HIV-1 infection (47). The expression of MX1 remains high in among people with HIV inflammation especially in females as well as the IFN-α production levels (48). Interferon-induced protein with tetratricopeptide repeat-1 (*IFIT1*) can restrict HIV replication in macrophages along with other family IFIT proteins affecting the size of HIV reservoir in macrophages (49).

The interferon-induced transmembrane protein 1 (*IFITM1*), strongly induced by the interferon family (mostly IFN-α and IFN- γ), encodes for the protein with the same name and is involved in inflammation (50). In the pathway enrichment test, this gene was mediated in the pathway of antiviral defense (FDR q-value 6.1×10^{-7}). IFITM1 also is essential to induce the suppression of the growth of tumor cells along with IFN- γ and *IFITM 1* can intermediate with

STAT1 and p53 signaling pathways with antiproliferation (51). Moreover, a study has confirmed the function of IFITM1 protein to inhibit the viral replication of HIV (52). These findings have proved the function *IFITM1* of inhibition of HIV replication and antiproliferation of tumor cells; therefore, *IFITM1* can potentially serve as a biomarker like *STAT1* for HIV therapeutic target in suppression or inhibition of viral replication.

Vacuole membrane protein 1 (*VMP1*) encodes a transmembrane protein located in the Golgi apparatus and endoplasmic reticulum leading autophagy in cells under overexpression of such proteins (53). Autophagy is crucial in the innate immune system isolating the microbial pathogens with catabolic process to clear out the pathogens in the lysosome (54). The way of stimulating autophagy-mediated lysosomal degradation can potentially strengthen the immune response to HIV (55). Our EWAS results showed one of the *VMP1* methylated site, cg16936953, most significantly associated with circulating IL-6 levels. This site showed the association with elevated IL-6 levels implying the demethylation is related with inflammation among PWH. The methylation on *VMP1* was also confirmed in the previous study among the patients with breast cancers exposing to the chemotherapy or not (32). Same CpG site (cg16936953) was reported in this study showing the decreased methylation of *VMP1* among the patients who received chemotherapy and the decreased methylation was associated with increased IL-6 plasma levels. The decreased methylation also mediated to increase in the inflammatory biomarkers like IL-6 adjusting for multiple clinical and treatment characteristics. *VMP1* methylation also has been confirmed its association with childhood-onset Crohn's Disease (56). Although the specific function of *VMP1* impacting autophagy after epigenetics alterations remains unknown among PWH, demethylation on *VMP1* has been confirmed in this EWAS associated with IL-6 plasma

levels among PWH. The future direction could be focused on the investigation the effect on autophagy of IL-6 demethylation.

Based on the results of the enrichment pathway test, the most significant pathway was identified as the type-1 interferon signaling pathway with several significant genes of *OSA3, STAT1*, *IFIT1*, *IFITM1*and *MX1.* These are the genes mediated with interferons which can induce antiviral states and inhibit viral replication by producing restriction factors during HIV infection (57). However, HIV developed a mechanism that can downregulate a number of interferons-induced genes including *OSA3* to cause the suppression of transcription of genes like *OSA3* (58). A recent study has revealed that the blockade interferon signaling pathways with ART treatment can restore the immune response in HIV infection especially for the chronic inflammation (59). *VMP1* gene is involved in innate immunity pathway which was also identified as one of the most significant pathways from the enrichment pathway test. The activation of the innate immune pathways is linked to the stronger adaptive immune responses with the activation of T cells during HIV infection (60). As mentioned previously, *VMP1* is associated with autophagy which can restrict HIV infection by degrading Tat, the protein in HIV-1 virus, in lymphocytes. Therefore, based on our EWAS findings of these methylated sites and the previous results, it further confirms that the interferon-mediated genes can potentially serve as the biomarkers in HIV chronic inflammation.

In our study, both 450K and EPIC arrays have replicated the top IL6-associated DNAm site with the most statistical significance in meta-analysis, cg16936953. However, there were still 11 DNAm sites which were statistically significant in EPIC array but not measured in 450K array. Therefore, for the future implications, we should expand our data resources to cover more

replication sites in both chips thus increasing the likelihood to find more IL6-associated DNAm sites among PWH.

There are still multiple limitations in our study. First, because two microarray platforms were used in the two sub-cohorts, only the commonly measured DNAm sites were included in the meta-analysis. Future replication and meta-analysis of many DNAm sites unique to the platform could reveal additional significant associations with IL-6. Second, the current EWAS focused on male PWH. If the DNAm sites are differentially associated with IL-6 between males and females with HIV, our results may not be generalizable in women with HIV. Moreover, majority of the study samples were African Americans, which may also limit the generalizability across other racial and ethnic groups. Based on our findings, future EWAS of IL-6 can be conducted in more diverse demographic characteristics using more comprehensive epi-typing methods to establish a more complete catalog of IL-6-associated DNAm sites across human genome, and to examine their roles in chronic disease progression, morbidities and mortality among PWH. Additionally, the genes and pathways of the top methylated genes were biologically relevant but cannot directly infer molecular function solely based on the cross-sectional association analyses. Such hypothesis-generating process can provide probably targets for future hypothesis-driven research using experimental approaches. Although the EPIC BeadChip measures the methylation levels of over 850,000 DNAm sites on human genome, the coverage can be improved by whole genome bisulfide sequencing to completely survey the human methylome. Inspired by robust findings in present EWAS of IL-6 levels, future EWAS can better address the role of IL-6 and other inflammatory biomarkers on chronic disease outcomes and mortality among PWH.

Conclusion

Our EWAS of IL-6 methylation has demonstrated statistically robust epigenetic associations among PWH. The results would be helpful to further investigate the pathogenesis of inflammation and can imply as a necessary accompaniment to study the chronic diseases and survival status of HIV infection. This EWAS can also potentially inform the therapeutic targets based on the discovered DNAm sites among PWH. Future directions from this EWAS could be expanded to the investigation of mechanisms of the IL-6 methylation sites on these discovered genes (*VMP1*, *IFITM1*, *STAT1*, *MX1* and *OSA1*) specifically linked to the chronic inflammation among PWH.

References:

1. Blood, G. A. C. (2016). Human immunodeficiency virus (HIV). *Transfusion Medicine and Hemotherapy*, *43*(3), 203.
2. Organization, W. H. (2019). *Progress report on HIV, viral hepatitis and sexually transmitted infections 2019: accountability for the global health sector strategies, 2016–2021*.
3. Villarosa, L. (2019). America's hidden HIV epidemic. In *The Social Medicine Reader, Volume II, Third Edition* (pp. 235-253): Duke University Press.
4. Gayle, H. D., & Hill, G. L. (2001). Global impact of human immunodeficiency virus and AIDS. Clin Microbiol Rev, 14(2), 327-335. doi:10.1128/cmr.14.2.327-335.2001
5. Piot, P., Bartos, M., Ghys, P. D., Walker, N., & Schwartländer, B. (2001). The global impact of HIV/AIDS. *Nature*, *410*(6831), 968-973.
6. Schooley, R. T., & Mellors, J. W. (2007). No cure yet for HIV-1, but therapeutic research presses on. *The Journal of infectious diseases*, *195*(6), 770-772.
7. Littlewood, R. A., & Vanable, P. A. (2008). *Complementary and alternative medicine use among HIV-positive people: research synthesis and implications for HIV care*. *AIDS care*, *20*(8), 1002-1018.
8. Farahat, F. M., Alghamdi, Y. S., Farahat, A. F., Alqurashi, A. A., Alburayk, A. K., Alabbasi, A. A., . . . Alshamrani, M. M. (2020). *The prevalence of comorbidities among adult people diagnosed with HIV infection in a tertiary care hospital in western Saudi Arabia*. *Journal of Infection and Public Health*, *13*(11), 1699-1704.
9. Taub, D., & Oppenheim, J. (1994). *Chemokines, inflammation and the immune system. Therapeutic immunology*, 1(4), 229-246.
10. Pahwa, R., Goyal, A., Bansal, P., & Jialal, I. (2021). *Chronic Inflammation*. In StatPearls. Treasure Island (FL): StatPearls Publishing Copyright © 2021, StatPearls Publishing LLC.
11. Appay, V., & Sauce, D. (2008). *Immune activation and inflammation in HIV-1 infection: causes and consequences*. The Journal of Pathology, 214(2), 231-241. doi:https://doi.org/10.1002/path.2276
12. Gonzalez-Jaramillo, V., Portilla-Fernandez, E., Glisic, M., Voortman, T., Ghanbari, M., Bramer, W., . . . Franco, O. H. (2019). *Epigenetics and inflammatory markers: a systematic review of the current evidence*. International journal of inflammation, 2019.
13. Deeks, S. G., Tracy, R., & Douek, D. C. (2013). *Systemic effects of inflammation on health during chronic HIV infection*. Immunity, 39(4), 633-645. doi:10.1016/j.immuni.2013.10.001
14. Hirano, T., Akira, S., Taga, T., & Kishimoto, T. (1990). *Biological and clinical aspects of interleukin 6. Immunology today*, 11, 443-449.
15. Nakagiri, T., Inoue, M., Minami, M., Shintani, Y., & Okumura, M. (2012). *Immunology mini-review: the basics of TH17 and interleukin-6 in transplantation.* Paper presented at the Transplantation proceedings.
16. Dardalhon, V., Korn, T., Kuchroo, V. K., & Anderson, A. C. (2008). Role of Th1 and Th17 cells in organ-specific autoimmunity. Journal of autoimmunity, 31(3), 252-256.
17. Breen, E. C., Rezai, A. R., Nakajima, K., Beall, G. N., Mitsuyasu, R. T., Hirano, T., . . . Martinez-Maza, O. (1990). *Infection with HIV is associated with elevated IL-6 levels and production. The Journal of Immunology*, 144(2), 480-484. Retrieved from https://www.jimmunol.org/content/jimmunol/144/2/480.full.pdf
18. Trovato, M., Ruggeri, R. M., Sciacchitano, S., Vicchio, T. M., Picerno, I., Pellicanò, G., . . . Visalli, G. (2018). Serum interleukin-6 levels are increased in HIV-infected patients that develop autoimmune disease during long-term follow-up. *Immunobiology*, *223*(3), 264-268. doi:https://doi.org/10.1016/j.imbio.2017.10.039
19. Borges, Á. H., O'Connor, J. L., Phillips, A. N., Rönsholt, F. F., Pett, S., Vjecha, M. J., . . . Lundgren, J. D. (2015). Factors associated with plasma IL-6 levels during HIV infection. *The Journal of infectious diseases*, *212*(4), 585-595.
20. Dinarello, C. A. (2000). Proinflammatory cytokines. *Chest*, *118*(2), 503-508.

21. Matuzkova, A., Pshenichnaya, N., Suladze, A., Tverdokhlebova, T., Dosyagaeva, L., & Zhuravlev, A. (2019). Markers of systemic inflammation in HIV-infected patients with different HIV RNA level. *International Journal of Infectious Diseases*, *79*, 85.
22. Borges Á, H., O'Connor, J. L., Phillips, A. N., Neaton, J. D., Grund, B., Neuhaus, J., . . . Lundgren, J. D. (2016). Interleukin 6 Is a Stronger Predictor of Clinical Events Than High-Sensitivity C-Reactive Protein or D-Dimer During HIV Infection. J Infect Dis, 214(3), 408-416. doi:10.1093/infdis/jiw173
23. Míguez, M. J., Rosenberg, R., Burbano-Levy, X., Carmona, T., & Malow, R. (2012). The effect of alcohol use on IL-6 responses across different racial/ethnic groups. *Future virology*, *7*(2), 205-213.
24. Gonzalez-Jaramillo, V., Portilla-Fernandez, E., Glisic, M., Voortman, T., Ghanbari, M., Bramer, W., . . . Franco, O. H. (2019). Epigenetics and inflammatory markers: a systematic review of the current evidence. International journal of inflammation, 2019.
25. Zhang, X., Justice, A. C., Hu, Y., Wang, Z., Zhao, H., Wang, G., . . . Krystal, J. H. (2016). Epigenome-wide differential DNA methylation between HIV-infected and uninfected individuals. Epigenetics, 11(10), 750-760.
26. Paschos, K., & Allday, M. J. (2010). Epigenetic reprogramming of host genes in viral and microbial pathogenesis. Trends in microbiology, 18(10), 439-447.
27. Chen, J., Huang, Y., Hui, Q., Mathur, R., Gwinn, M., So-Armah, K., . . . Sun, Y. V. (2020). Epigenetic Associations With Estimated Glomerular Filtration Rate Among Men With Human Immunodeficiency Virus Infection. Clin Infect Dis, 70(4), 667-673. doi:10.1093/cid/ciz240
28. Sun, Y. V., Lazarus, A., Smith, J. A., Chuang, Y.-H., Zhao, W., Turner, S. T., & Kardia, S. L. (2013). Gene-specific DNA methylation association with serum levels of C-reactive protein in African Americans. PloS one, 8(8), e73480.
29. Verschoor, C. P., McEwen, L. M., Kobor, M. S., Loeb, M. B., & Bowdish, D. M. (2018). DNA methylation patterns are related to co-morbidity status and circulating C-reactive protein levels in the nursing home elderly. Experimental gerontology, 105, 47-52.
30. Verschoor, C. P., McEwen, L. M., Kohli, V., Wolfson, C., Bowdish, D. M., Raina, P., . . . Balion, C. (2017). The relation between DNA methylation patterns and serum cytokine levels in community-dwelling adults: a preliminary study. BMC genetics, 18(1), 1-7.
31. Uddin, M., Koenen, K. C., Aiello, A. E., Wildman, D. E., de los Santos, R., & Galea, S. (2011). Epigenetic and inflammatory marker profiles associated with depression in a community-based epidemiologic sample. *Psychol Med, 41*(5), 997-1007. doi:10.1017/s0033291710001674
32. Smith, A. K., Conneely, K. N., Pace, T. W., Mister, D., Felger, J. C., Kilaru, V., . . . Torres, M. A. (2014). Epigenetic changes associated with inflammation in breast cancer patients treated with chemotherapy. *Brain, behavior, and immunity*, *38*, 227-236.
33. Nordan, R. P., Richards, C. D., & Gauldie, J. (2001). Measurement of interleukin-6. Curr Protoc Immunol, Chapter 6, Unit 6.6. doi:10.1002/0471142735.im0606s17
34. Zhang, X., Hu, Y., Justice, A. C., Li, B., Wang, Z., Zhao, H., . . . Xu, K. (2017). DNA methylation signatures of illicit drug injection and hepatitis C are associated with HIV frailty. Nature Communications, 8(1), 2243. doi:10.1038/s41467-017-02326-1
35. Solomon O, MacIsaac J, Quach H, et al. Comparison of DNA methylation measured by Illumina 450K and EPIC BeadChips in blood of newborns and 14-year-old children. Epigenetics 2018;13:655-64.
36. Mathur, R., Hui, Q., Huang, Y., Gwinn, M., So-Armah, K., Freiberg, M. S., . . . Sun, Y. V. (2019). DNA methylation markers of type 2 diabetes mellitus among male veterans with or without human immunodeficiency virus infection. The Journal of infectious diseases, 219(12), 1959-1962.
37. Houseman, E. A., Accomando, W. P., Koestler, D. C., Christensen, B. C., Marsit, C. J., Nelson, H. H., . . . Kelsey, K. T. (2012). DNA methylation arrays as surrogate measures of cell mixture distribution. BMC bioinformatics, 13(1), 86. doi:10.1186/1471-2105-13-86
38. Chmurzynska, A., Muzsik, A., Krzyżanowska-Jankowska, P., Walkowiak, J., & Bajerska, J. (2019). The effect of habitual fat intake, IL6 polymorphism, and different diet strategies on inflammation in postmenopausal women with central obesity. *Nutrients*, *11*(7), 1557.

39. Hunt, P. W. (2012). HIV and inflammation: mechanisms and consequences. *Current HIV/AIDS Reports, 9*(2), 139-147.
40. Huang, D. W., Sherman, B. T., & Lempicki, R. A. (2009). Systematic and integrative analysis of large gene lists using DAVID bioinformatics resources. Nature Protocols, 4(1), 44-57. doi:10.1038/nprot.2008.211
41. Baris, S., Alroqi, F., Kiykim, A., Karakoc-Aydiner, E., Ogulur, I., Ozen, A., . . . Barlan, I. B. (2016). Severe Early-Onset Combined Immunodeficiency due to Heterozygous Gain-of-Function Mutations in STAT1. *J Clin Immunol, 36*(7), 641-648. doi:10.1007/s10875-016-0312-3
42. Chaudhuri, A., Yang, B., Gendelman, H. E., Persidsky, Y., & Kanmogne, G. D. (2008). STAT1 signaling modulates HIV-1-induced inflammatory responses and leukocyte transmigration across the blood-brain barrier. *Blood, 111*(4), 2062-2072. doi:10.1182/blood-2007-05-091207
43. Tanabe, K., Matsushima-Nishiwaki, R., Yamaguchi, S., Iida, H., Dohi, S., & Kozawa, O. (2010). Mechanisms of tumor necrosis factor-alpha-induced interleukin-6 synthesis in glioma cells. J Neuroinflammation, 7, 16. doi:10.1186/1742-2094-7-16
44. Li, Y., Banerjee, S., Wang, Y., Goldstein, S. A., Dong, B., Gaughan, C., . . . Weiss, S. R. (2016). Activation of RNase L is dependent on OAS3 expression during infection with diverse human viruses. Proceedings of the National Academy of Sciences, 113(8), 2241-2246. doi:10.1073/pnas.1519657113
45. Rogez-Kreuz, C., Manéglier, B., Martin, M., Dereuddre-Bosquet, N., Martal, J., Dormont, D., & Clayette, P. (2005). Involvement of IL-6 in the anti-human immunodeficiency virus activity of IFN-τ in human macrophages. International Immunology, 17(8), 1047-1057. doi:10.1093/intimm/dxh285
46. Pavlovic, J., Zürcher, T., Haller, O., & Staeheli, P. (1990). Resistance to influenza virus and vesicular stomatitis virus conferred by expression of human MxA protein. J Virol, 64(7), 3370-3375. doi:10.1128/jvi.64.7.3370-3375.1990
47. Hofer, U. (2013). Interfering with HIV infection. Nature Reviews Microbiology, 11(11), 743-743. doi:10.1038/nrmicro3145
48. Chang, J. J., Woods, M., Lindsay, R. J., Doyle, E. H., Griesbeck, M., Chan, E. S., . . . Altfeld, M. (2013). Higher expression of several interferon-stimulated genes in HIV-1-infected females after adjusting for the level of viral replication. J Infect Dis, 208(5), 830-838. doi:10.1093/infdis/jit262
49. Nasr, N., Alshehri, A. A., Wright, T. K., Shahid, M., Heiner, B. M., Harman, A. N., . . . Cunningham, A. L. (2017). Mechanism of Interferon-Stimulated Gene Induction in HIV-1-Infected Macrophages. J Virol, 91(20). doi:10.1128/jvi.00744-17
50. Kim, S. H., In Choi, H., Choi, M. R., An, G. Y., Binas, B., Jung, K. H., & Chai, Y. G. (2020). Epigenetic regulation of IFITM1 expression in lipopolysaccharide-stimulated human mesenchymal stromal cells. Stem Cell Research & Therapy, 11(1), 16. doi:10.1186/s13287-019-1531-3
51. Yang, G., Xu, Y., Chen, X., & Hu, G. (2007). IFITM1 plays an essential role in the antiproliferative action of interferon-gamma. Oncogene, 26(4), 594-603. doi:10.1038/sj.onc.1209807
52. Lu, J., Pan, Q., Rong, L., Liu, S.-L., & Liang, C. (2011). The IFITM Proteins Inhibit HIV-1 Infection. Journal of Virology, 85(5), 2126-2137. doi:10.1128/jvi.01531-10
53. Jiang, G.-M., Tan, Y., Wang, H., Peng, L., Chen, H.-T., Meng, X.-J., . . . Shan, H. (2019). The relationship between autophagy and the immune system and its applications for tumor immunotherapy. Molecular Cancer, 18(1), 17. doi:10.1186/s12943-019-0944-z
54. Germic, N., Frangez, Z., Yousefi, S., & Simon, H. U. (2019). Regulation of the innate immune system by autophagy: monocytes, macrophages, dendritic cells and antigen presentation. *Cell Death Differ, 26*(4), 715-727. doi:10.1038/s41418-019-0297-6
55. Nardacci, R., Ciccosanti, F., Marsella, C., Ippolito, G., Piacentini, M., & Fimia, G. M. (2017). Role of autophagy in HIV infection and pathogenesis. *J Intern Med, 281*(5), 422-432. doi:10.1111/joim.12596
56. Adams, A. T., Kennedy, N. A., Hansen, R., Ventham, N. T., O'Leary, K. R., Drummond, H. E., . . . Satsangi, J. (2014). Two-stage genome-wide methylation profiling in childhood-onset Crohn's Disease implicates epigenetic alterations at the VMP1/MIR21 and HLA loci. *Inflamm Bowel Dis, 20*(10), 1784-1793. doi:10.1097/mib.0000000000000179

57. Nganou-Makamdop, K., & Douek, D. C. (2019). Manipulating the Interferon Signaling Pathway: Implications for HIV Infection. *Virol Sin, 34*(2), 192-196. doi:10.1007/s12250-019-00085-5
58. He, B., Tran, J. T., & Sanchez, D. J. (2019). Manipulation of Type I Interferon Signaling by HIV and AIDS-Associated Viruses. Journal of Immunology Research, 2019, 8685312. doi:10.1155/2019/8685312
59. Zhen, A., Rezek, V., Youn, C., Lam, B., Chang, N., Rick, J., . . . Kitchen, S. G. (2017). Targeting type I interferon-mediated activation restores immune function in chronic HIV infection. J Clin Invest, 127(1), 260-268. doi:10.1172/jci89488
60. Altfeld, M., & Gale Jr, M. (2015). Innate immunity against HIV-1 infection. *Nature Immunology, 16*(6), 554-562. doi:10.1038/ni.3157

Tables

Table 1. Phenotypic Characteristics of two subsets of VACS cohort in the EWAS of interleukin 6.

Variable	EPIC (n=490)	450K (n=512)	P-values
Race			0.217
Black, %	396 (80.8)	430 (84.0)	
Non-Black, %	94 (19.2)	82 (16.0)	
Smoking, Yes, %	376 (76.7)	408 (79.7)	0.291
Virus Load, < 75, %	212 (43.3)	230 (44.9)	0.376
Age, years	51.5 (7.7)	52.1 (7.8)	0.256
BMI, kg/m^2	26.2 (5.1)	25.7 (4.8)	0.088
ART, Yes, %	411 (83.9)	432 (83.4)	0.897
Alcohol use, Abuse, %	294 (60.0)	214 (41.8)	0.314
Diabetes, Yes, %	90 (18.4)	93 (18.2)	0.999
HBV, Positive, %	39 (8.0)	52 (10.2)	0.452
HCV, Positive, %	175 (35.7)	248 (48.4)	$<5.43\times 10^{-13}$
IL-6 (pg/mL)	2.20 (1.20)	2.40 (1.40)	0.174
CD4 Counts	455 (274)	433 (280)	0.218
CD4 T cell proportion	0.07 (0.05)	0.10 (0.05)	2.61×10^{-13}
CD8 Counts	978 (508)	973 (526)	0.882
CD8 T cell proportion	0.28 (0.09)	0.15 (0.07)	$<2.20\times 10^{-16}$
NK Cell proportion	0.006 (0.012)	0.10 (0.05)	$<2.20\times 10^{-16}$
B Cell proportion	0.09 (0.04)	0.10 (0.05)	6.06×10^{-4}
Monocytes proportion	0.15 (0.03)	0.11 (0.04)	$<2.20\times 10^{-16}$
Granules proportion	0.45 (0.10)	0.50 (0.12)	5.26×10^{-14}

**abbreviation: HBV: Hepatitis B virus; HCV: Hepatitis C virus; ART: Antiretroviral Therapy; IL6: Interleukin 6.*

Table 2. Summary statistics of top 20 DNAm sites from the meta-analysis of IL-6 EWAS.

Chromosome location			**Annotated Gene Name**	**Meta-analysis**			450K **dataset**			EPIC (850K) dataset		
CPG ID	CHR	Base pair		**Beta**	**SE**	**P-value**	**Beta**	**SE**	**P-value**	**Beta**	**SE**	**P-value**
cg16936953	17	57915665	*VMP1*	-1.92×10^{-2}	2.12×10^{-3}	8.83×10^{-21}	-2.06×10^{-2}	2.75×10^{-3}	4.90×10^{-13}	-1.77×10^{-2}	3.15×10^{-3}	4.14×10^{-8}
cg23570810	11	315102	*IFITM1*	-2.01×10^{-2}	2.45×10^{-3}	2.01×10^{-18}	-2.01×10^{-2}	3.13×10^{-3}	3.94×10^{-10}	-2.19×10^{-2}	3.68×10^{-3}	7.13×10^{-9}
cg01971407	11	313624	*IFITM1*	-1.33×10^{-2}	1.60×10^{-3}	5.03×10^{-18}	-1.33×10^{-2}	2.18×10^{-3}	3.05×10^{-9}	-1.38×10^{-2}	2.23×10^{-3}	2.22×10^{-9}
cg18942579	17	57915773	*VMP1*	-1.36×10^{-2}	1.60×10^{-3}	9.90×10^{-17}	-1.34×10^{-2}	1.98×10^{-2}	5.55×10^{-11}	-1.37×10^{-2}	2.84×10^{-3}	2.15×10^{-6}
cg03038262	11	315262	*IFITM1*	-1.61×10^{-2}	2.02×10^{-3}	4.43×10^{-16}	-1.66×10^{-2}	2.69×10^{-3}	1.80×10^{-9}	-1.68×10^{-2}	2.99×10^{-2}	2.32×10^{-7}
cg10552523	11	313478	*IFITM1*	-1.52×10^{-2}	1.92×10^{-3}	1.22×10^{-15}	-1.49×10^{-2}	2.61×10^{-3}	2.17×10^{-8}	-1.57×10^{-2}	2.81×10^{-3}	4.92×10^{-8}
cg07839457	16	57023022	*NA*	-2.39×10^{-2}	3.10×10^{-3}	7.26×10^{-15}	-2.23×10^{-2}	4.26×10^{-3}	2.69×10^{-7}	-2.55×10^{-2}	4.42×10^{-3}	1.88×10^{-8}
cg08122652	3	122281939	*PARP9; DTX3L*	-2.41×10^{-2}	3.10×10^{-2}	1.21×10^{-14}	-2.20×10^{-2}	4.06×10^{-3}	1.07×10^{-7}	-2.72×10^{-2}	4.90×10^{-3}	6.12×10^{-8}
cg01409343	17	57915740	*VMP1*	-0.01	1.30×10^{-2}	1.70×10^{-14}	-1.13×10^{-2}	1.70×10^{-3}	1.13×10^{-12}	-8.20×10^{-3}	2.03×10^{-3}	7.31×10^{-5}
cg26470501	19	45252955	*BCL3*	-7.20×10^{-3}	9.00×10^{-4}	1.98×10^{-14}	-7.30×10^{-3}	1.29×10^{-3}	2.79×10^{-8}	-7.10×10^{-3}	1.39×10^{-3}	5.06×10^{-7}
cg22930808	3	122281881	*PARP9; DTX3L*	-2.90×10^{-2}	3.90×10^{-3}	8.26×10^{-14}	-2.1×10^{-2}	5.26×10^{-3}	6.22×10^{-6}	-3.47×10^{-2}	5.74×10^{-3}	4.13×10^{-9}
cg08818207	6	32820355	*TAP1*	-1.38×10^{-2}	1.80×10^{-2}	8.37×10^{-14}	-1.25×10^{-3}	2.50×10^{-3}	8.50×10^{-7}	-1.53×10^{-2}	2.74×10^{-3}	5.06×10^{-8}
cg00533183	6	32810742	*PSMB8-AS1*	-6.6×10^{-3}	9.00×10^{-4}	3.04×10^{-12}	-5.89×10^{-3}	1.15×10^{-3}	4.06×10^{-7}	-8.00×10^{-3}	1.67×10^{-3}	2.39×10^{-6}
cg00676801	2	191876673	*STAT1*	-7.70×10^{-3}	1.10×10^{-2}	3.81×10^{-12}	-6.58×10^{-3}	1.36×10^{-3}	1.83×10^{-6}	-1.00×10^{-2}	1.93×10^{-3}	4.12×10^{-7}
cg08099136	6	32811251	*PSMB8-AS1*	-1.08×10^{-2}	1.60×10^{-3}	5.81×10^{-12}	-7.66×10^{-3}	2.07×10^{-3}	2.24×10^{-4}	-1.49×10^{-2}	2.40×10^{-3}	1.60×10^{-9}
cg01082299	6	31431969	*HCP5*	-1.27×10^{-2}	1.80×10^{-3}	5.86×10^{-12}	-9.59×10^{-3}	2.40×10^{-3}	7.62×10^{-5}	-1.71×10^{-2}	2.88×10^{-3}	7.31×10^{-9}
cg12054453	17	57915717	*VMP1*	-1.54×10^{-2}	2.20×10^{-3}	6.77×10^{-12}	-1.67×10^{-2}	3.04×10^{-3}	7.57×10^{-8}	-1.38×10^{-2}	3.32×10^{-3}	3.98×10^{-5}
cg22862003	21	42797588	*MX1*	-2.10×10^{-2}	3.10×10^{-3}	1.65×10^{-11}	-1.62×10^{-2}	4.12×10^{-3}	9.96×10^{-5}	-2.75×10^{-2}	4.78×10^{-3}	2.14×10^{-8}
cg08998192	6	32805570	*TAP2*	-8.20×10^{-2}	1.20×10^{-3}	2.97×10^{-11}	-7.17×10^{-3}	1.69×10^{-3}	2.78×10^{-5}	-9.20×10^{-3}	1.78×10^{-3}	3.87×10^{-7}
cg06981309	3	146260954	*PLSCR1*	-1.78×10^{-2}	2.70×10^{-3}	4.16×10^{-11}	-1.66×10^{-2}	3.52×10^{-3}	3.57×10^{-6}	-1.95×10^{-2}	4.18×10^{-3}	4.81×10^{-6}

**SE: standard error; NA: Not applicable*

Table 3. Summary of Top Significant Biological Pathways of the 81 unique genes from Meta-Analysis from Pathway Enrichment Analysis by DAVID test.

Biological Process (with Benjamini p-value)	Gene list
Type-1 Interferon Signaling Pathway (p-value=1.9×10^{-11})	OAS3 MX1 IFI27 IFIT1 IRF1 HLA-A HLA-B HLA-E HLA-F STAT1
Antiviral Defense (p-value=6.1×10^{-7})	OAS3 DDX60 MX1 IFI44L IFIT1 IFITM1 IRF7 PLSCR1 STAT1
Response to Virus (p-value=2.0×10^{-6})	OAS3 BCL3 DDX60 MX1 IFI44 IFIT1 IFITM1 IRF7 ODC1
Immunity (p-value=5.4×10^{-6})	OAS3 DDX60 MX1 AIM2 IFIT1 IFITM1 IRF7 HLA-A

Antigen Processing and Presentation of Peptide Antigen via MHC Class I (p-value=1.3×10^{-5})	HLA-B HLA-E HLA-F TAP1 TAP2
Interferon-Gamma (IFN-γ) Mediated Signaling Pathway (p-value=3.2×10^{-5})	HLA-A HLA-B HLA-E HLA-F TAP1 TAP2 OAS3 IRF7
Defense Response to Virus (p-value=2.7×10^{-4})	HLA-A HLA-B HLA-E HLA-F STAT1 OAS3 DDX60 MX1 IFI44L IFIT1 IFITM1 PLSCR4 STAT1
Negative Regulation of Viral Genome Replication (p-value=9.8×10^{-4})	OAS3 MX1 IFITM1 IFITM1 PLSCR4
Innate Immunity (p-value=7.7×10^{-3})	OAS3 DDX60 MX1 AIM2 IFIT1 IFITM1 IRF7

Figures

Figure 1. Manhattan plot of the meta-analysis of IL-6 EWAS using 356,071 autosomal DNA methylation sites. The DNA methylation sites are ordered by chromosomal base-pair positions. The horizontal line indicates Bonferroni corrected p-value of 0.05 (nominal p-value of 1.40×10^{-7}).

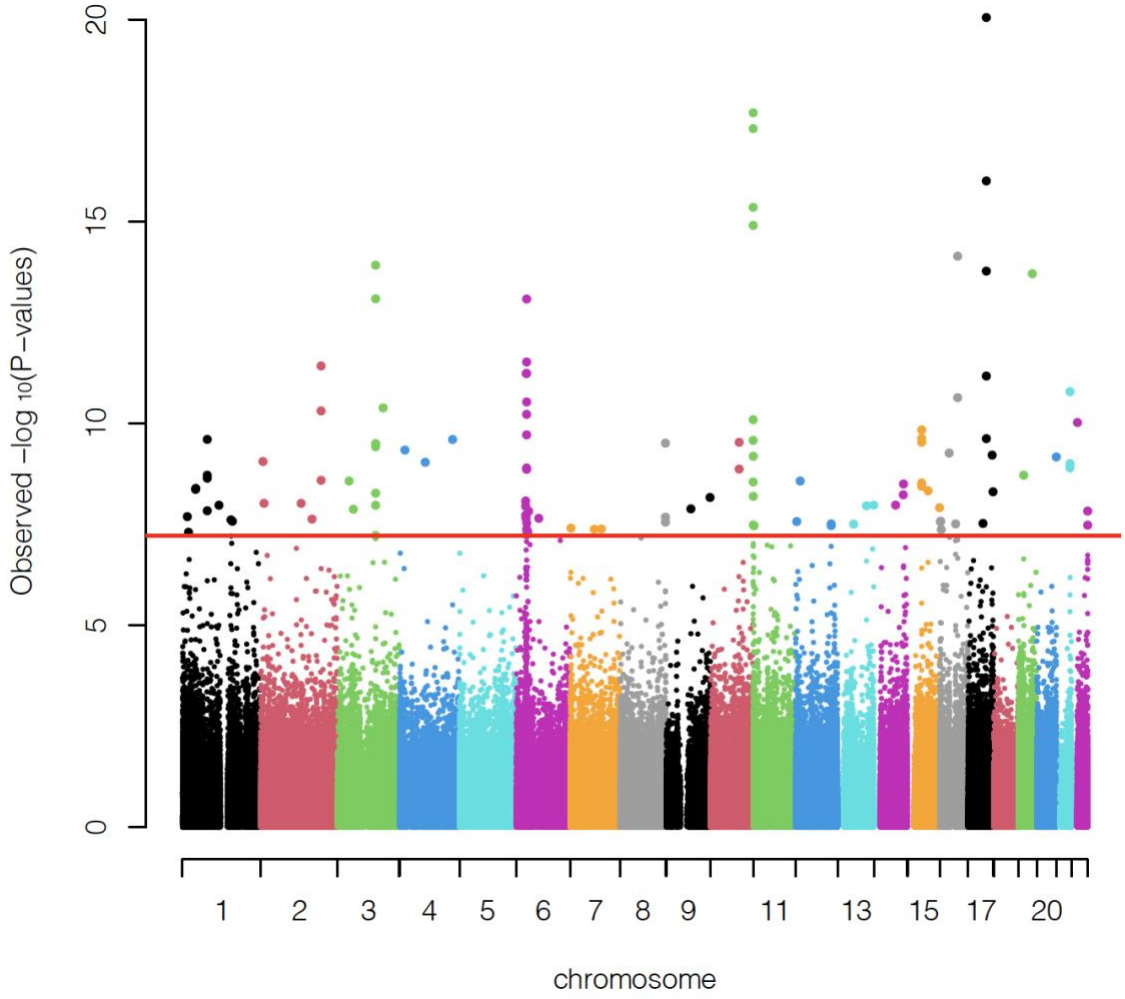

Figure 2. Quantile-quantile (Q-Q) plot of the meta-analysis of IL-6 EWAS using 356,071 autosomal DNA methylation sites.

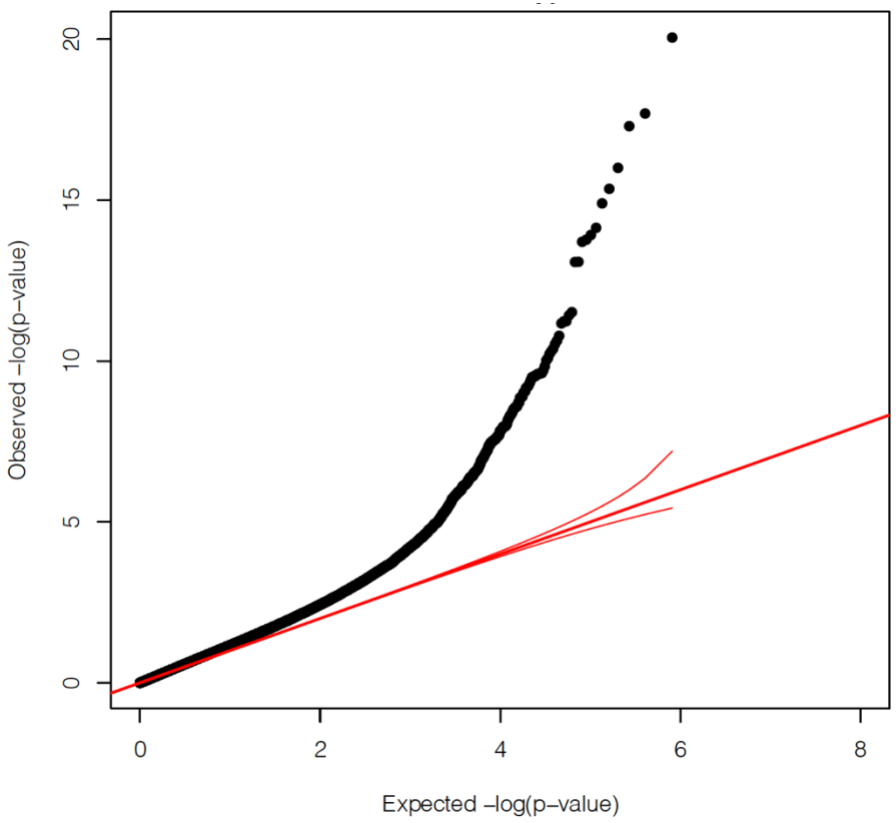

Figure 3. Comparison of effect sizes between 450K and EPIC subsets among 111 CpG sites significantly associated with IL-6 levels in the Meta-analysis

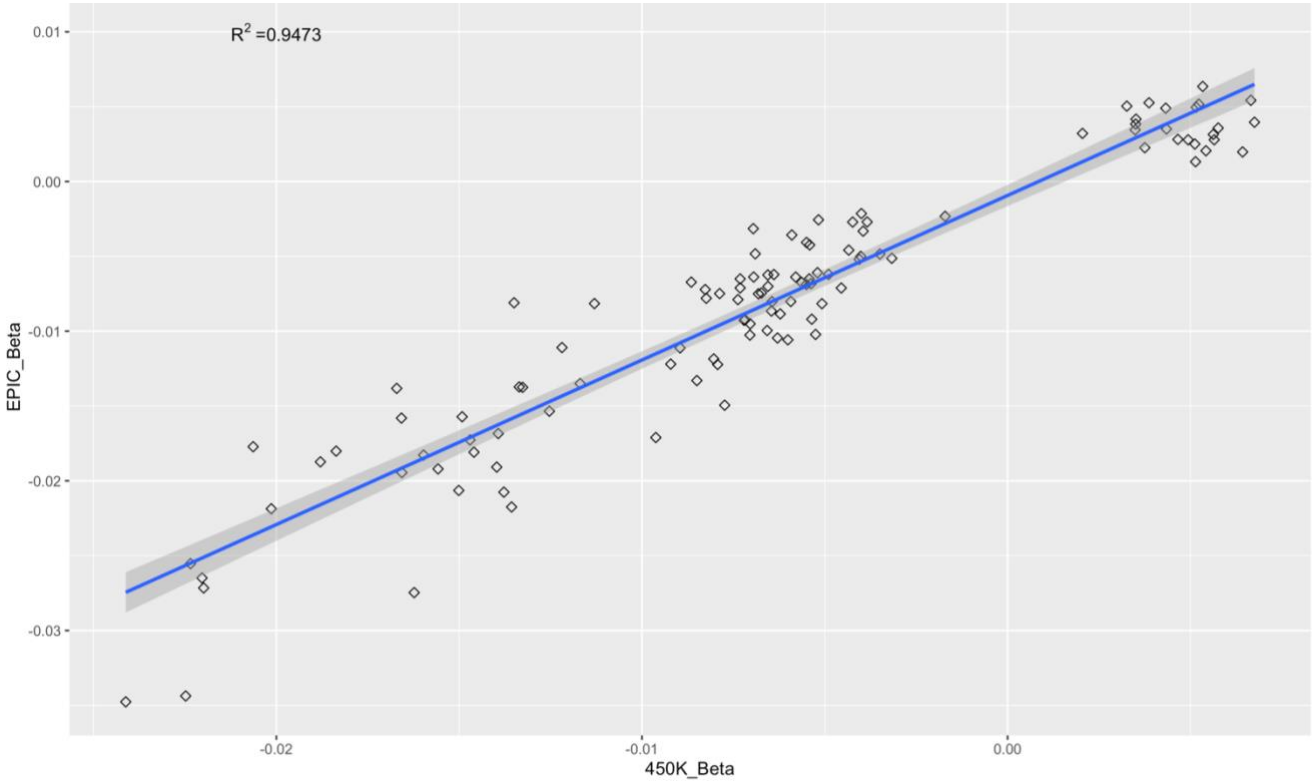

Supplementary Figures

Supplementary Figure 1A. Manhattan plot of EPIC EWAS

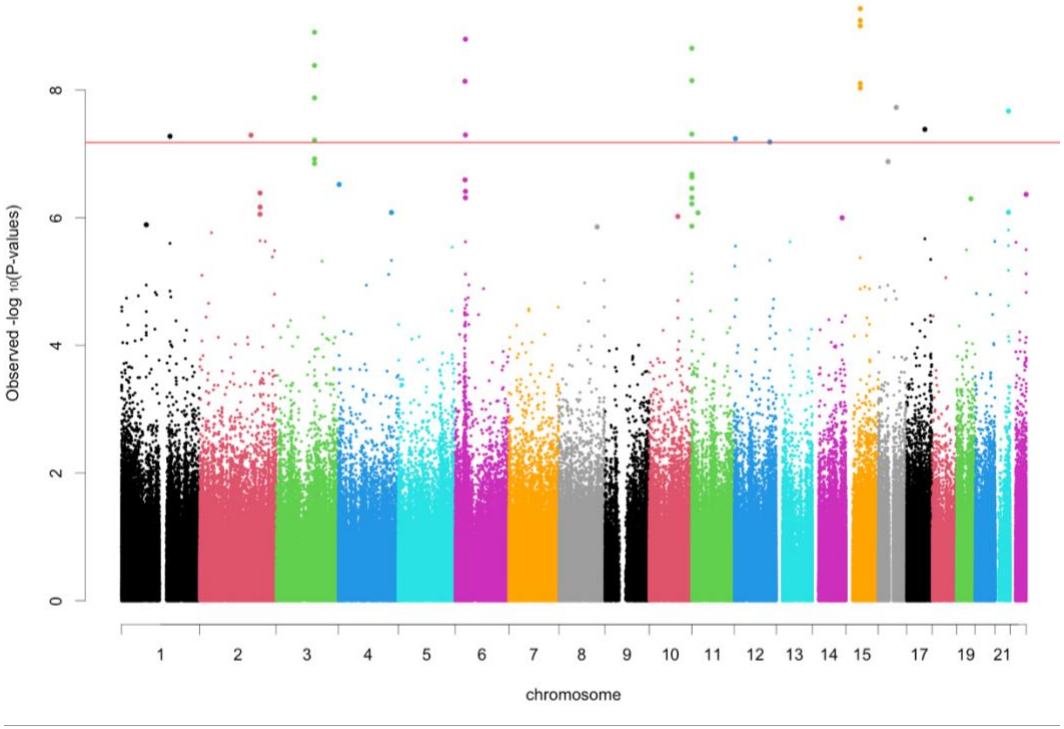

Supplementary Figure 1B. quantile-quantile plot of EPIC EWAS

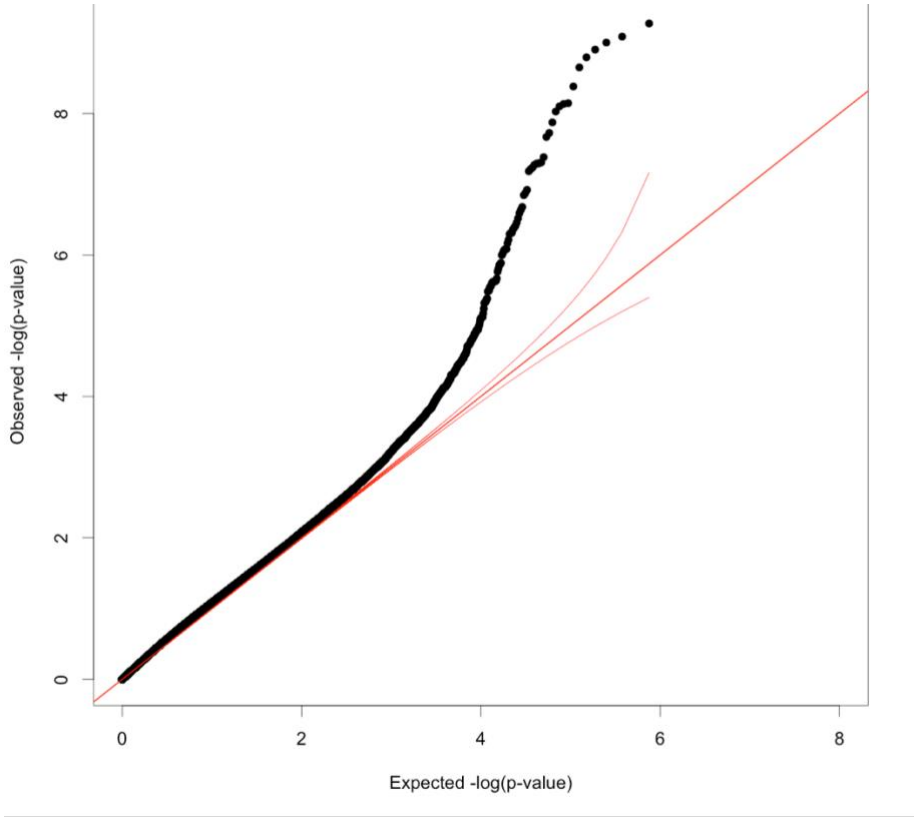

Supplementary Figure 2A. Manhattan plot of 450K EWAS

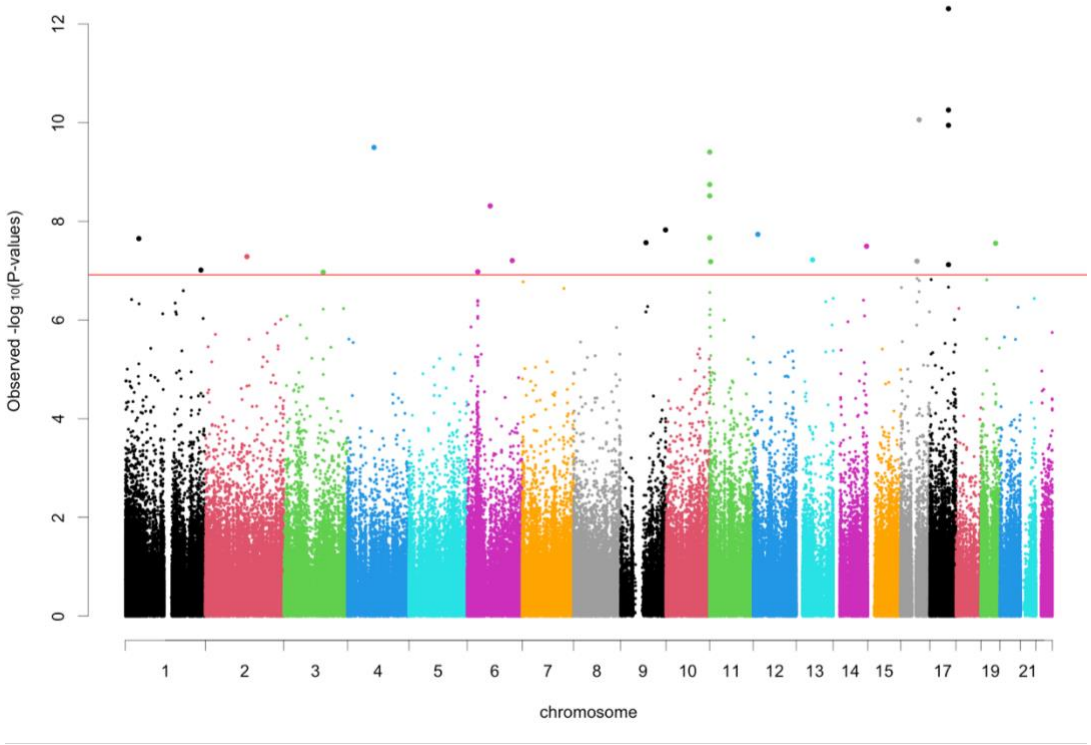

Supplementary Figure 2B. quantile-quantile plot of 450K EWAS

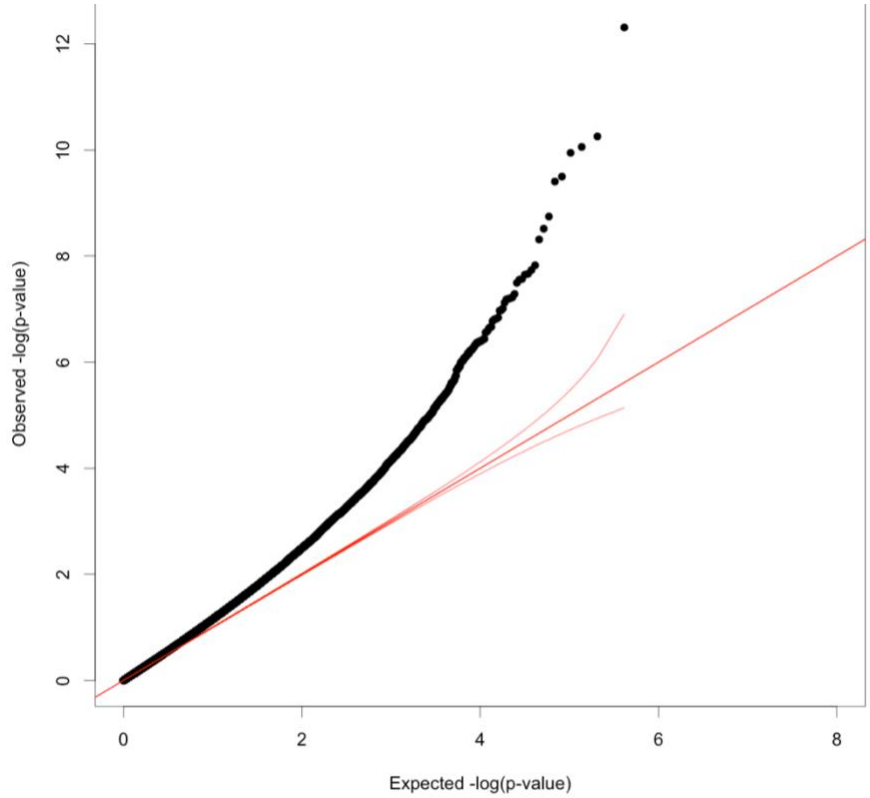

Supplementary Tables

Supplementary Table 1. Comparison of significant circulating IL6 associations between EPIC and 450K EWAS.

Measurement of significant EPIC EWAS in 450K subset	
Total number of significant DNAm sites in EPIC EWAS	22
Total number of significant DNAm sites measured in 450K	11 (50%)
Consistent direction of beta coefficients	11 (100 %)
Nominal p<0.05 in 450K	11 (100 %)
Bonferroni corrected p<0.05 in 450K	5 (45.5 %)
Measurement of significant 450K EWAS in EPIC subset	
Total number of significant DNAm sites in 450K EWAS	25
Total number of significant DNAm sites measured in EPIC	19 (76%)
Consistent direction in beta coefficient	19 (100 %)
Nominal p<0.05 in EPIC	12 (63.2 %)
Bonferroni corrected p<0.05 in EPIC	4 (21.1 %)

Supplementary Table 2. Summary statistics of top 20 IL6-associated DNAm sites from the meta-analysis of EPIC and 450K EWAS

Chromosome location			**Annotated Gene Name**	**Meta-analysis**			450K **dataset**			EPIC dataset		
CPG ID	CHR	Base pair		**Beta**	**SE**	**P-value**	**Beta**	**SE**	**P-value**	**Beta**	**SE**	**P-value**
cg16936953	17	57915665	*VMP1*	-1.92× 10^{-2}	2.12× 10^{-3}	8.83× 10^{-21}	-2.06× 10^{-2}	2.75× 10^{-3}	4.90× 10^{-13}	-1.77× 10^{-2}	3.15× 10^{-3}	4.14× 10^{-8}
cg23570810	11	315102	*IFITM1*	-2.01× 10^{-2}	2.45× 10^{-3}	2.01× 10^{-18}	-2.01× 10^{-2}	3.13× 10^{-3}	3.94× 10^{-10}	-2.19× 10^{-2}	3.68× 10^{-3}	7.13× 10^{-9}
cg01971407	11	313624	*IFITM1*	-1.33× 10^{-2}	1.60× 10^{-3}	5.03× 10^{-18}	-1.33× 10^{-2}	2.18× 10^{-3}	3.05× 10^{-9}	-1.38× 10^{-2}	2.23× 10^{-3}	2.22× 10^{-9}
cg18942579	17	57915773	*VMP1*	-1.36× 10^{-2}	1.60× 10^{-3}	9.90× 10^{-17}	-1.34× 10^{-2}	1.98× 10^{-2}	5.55× 10^{-11}	-1.37× 10^{-2}	2.84× 10^{-3}	2.15× 10^{-6}
cg03038262	11	315262	*IFITM1*	-1.61× 10^{-2}	2.02× 10^{-3}	4.43× 10^{-16}	-1.66× 10^{-2}	2.69× 10^{-3}	1.80× 10^{-9}	-1.68× 10^{-2}	2.99× 10^{-2}	2.32× 10^{-7}
cg10552523	11	313478	*IFITM1*	-1.52× 10^{-2}	1.92× 10^{-3}	1.22× 10^{-15}	-1.49× 10^{-2}	2.61× 10^{-3}	2.17× 10^{-8}	-1.57× 10^{-2}	2.81× 10^{-3}	4.92× 10^{-8}
cg07839457	16	57023022	*NA*	-2.39× 10^{-2}	3.10× 10^{-3}	7.26× 10^{-15}	-2.23× 10^{-2}	4.26× 10^{-3}	2.69× 10^{-7}	-2.55× 10^{-2}	4.42× 10^{-3}	1.88× 10^{-8}
cg08122652	3	122281939	*PARP9;DTX3L*	-2.41× 10^{-2}	3.10× 10^{-2}	1.21× 10^{-14}	-2.20× 10^{-2}	4.06× 10^{-3}	1.07× 10^{-7}	-2.72× 10^{-2}	4.90× 10^{-3}	6.12× 10^{-8}
cg01409343	17	57915740	*VMP1*	-0.01	1.30× 10^{-2}	1.70× 10^{-14}	-1.13× 10^{-2}	1.70× 10^{-3}	1.13× 10^{-12}	-8.20× 10^{-3}	2.03× 10^{-3}	7.31× 10^{-5}
cg26470501	19	45252955	*BCL3*	-7.20× 10^{-3}	9.00× 10^{-4}	1.98× 10^{-14}	-7.30× 10^{-3}	1.29× 10^{-3}	2.79× 10^{-8}	-7.10× 10^{-3}	1.39× 10^{-3}	5.06× 10^{-7}
cg22930808	3	122281881	*PARP9;DTX3L*	-2.90× 10^{-2}	3.90× 10^{-3}	8.26× 10^{-14}	-2.1× 10^{-2}	5.26× 10^{-3}	6.22× 10^{-6}	-3.47× 10^{-2}	5.74× 10^{-3}	4.13× 10^{-9}
cg08818207	6	32820355	*TAP1*	-1.38× 10^{-2}	1.80× 10^{-2}	8.37× 10^{-14}	-1.25× 10^{-3}	2.50× 10^{-3}	8.50× 10^{-7}	-1.53× 10^{-2}	2.74× 10^{-3}	5.06× 10^{-8}
cg00533183	6	32810742	*PSMB8-AS1*	-6.6× 10^{-3}	9.00× 10^{-4}	3.04× 10^{-12}	-5.89× 10^{-3}	1.15× 10^{-3}	4.06× 10^{-7}	-8.00× 10^{-3}	1.67× 10^{-3}	2.39× 10^{-6}
cg00676801	2	191876673	*STAT1*	-7.70× 10^{-3}	1.10× 10^{-2}	3.81× 10^{-12}	-6.58× 10^{-3}	1.36× 10^{-3}	1.83× 10^{-6}	-1.00× 10^{-2}	1.93× 10^{-3}	4.12× 10^{-7}
cg08099136	6	32811251	*PSMB8-AS1*	-1.08× 10^{-2}	1.60× 10^{-3}	5.81× 10^{-12}	-7.66× 10^{-3}	2.07× 10^{-3}	2.24× 10^{-4}	-1.49× 10^{-2}	2.40× 10^{-3}	1.60× 10^{-9}
cg01082299	6	31431969	*HCP5*	-1.27× 10^{-2}	1.80× 10^{-3}	5.86× 10^{-12}	-9.59× 10^{-3}	2.40× 10^{-3}	7.62× 10^{-5}	-1.71× 10^{-2}	2.88× 10^{-3}	7.31× 10^{-9}
cg12054453	17	57915717	*VMP1*	-1.54× 10^{-2}	2.20× 10^{-3}	6.77× 10^{-12}	-1.67× 10^{-2}	3.04× 10^{-3}	7.57× 10^{-8}	-1.38× 10^{-2}	3.32× 10^{-3}	3.98× 10^{-5}
cg22862003	21	42797588	*MX1*	-2.10× 10^{-2}	3.10× 10^{-3}	1.65× 10^{-11}	-1.62× 10^{-2}	4.12× 10^{-3}	9.96× 10^{-5}	-2.75× 10^{-2}	4.78× 10^{-3}	2.14× 10^{-8}
cg08998192	6	32805570	*TAP2*	-8.20× 10^{-2}	1.20× 10^{-3}	2.97× 10^{-11}	-7.17× 10^{-3}	1.69× 10^{-3}	2.78× 10^{-5}	-9.20× 10^{-3}	1.78× 10^{-3}	3.87× 10^{-7}
cg06981309	3	146260954	*PLSCR1*	-1.78× 10^{-2}	2.70× 10^{-3}	4.16× 10^{-11}	-1.66× 10^{-2}	3.52× 10^{-3}	3.57× 10^{-6}	-1.95× 10^{-2}	4.18× 10^{-3}	4.81× 10^{-6}
cg14951497	2	191875807	*STAT1*	-7.60× 10^{-3}	1.20× 10^{-3}	4.95× 10^{-11}	-6.29× 10^{-3}	1.38× 10^{-3}	6.94× 10^{-6}	-1.05× 10^{-2}	2.08× 10^{-3}	8.82× 10^{-7}
cg01309328	**6**	**32811253**	*PSMB8-AS1*	-0.0095	0.0015	6.01× 10^{-11}	-0.00793	0.00185	2.24× 10^{-5}	-0.0122	0.00238	4.88× 10^{-7}

cg09026253	**11**	**313267**	*IFITM1*	-9.60× 10^{-3}	1.50× 10^{-3}	8.16× 10^{-11}	-8.04× 10^{-3}	1.90× 10^{-3}	2.96× 10^{-5}	=1.19× 10^{-2}	2.33× 10^{-3}	6.08× 10^{-7}
cg14293575	**22**	**18635460**	*USP18*	-1.71× 10^{-2}	2.60× 10^{-3}	9.60× 10^{-11}	-1.50× 10^{-2}	3.36× 10^{-3}	1.08× 10^{-5}	-2.06× 10^{-2}	4.30× 10^{-3}	2.44× 10^{-6}
cg22940798	**6**	**32805554**	*TAP2*	8.10× 10^{-3}	1.30× 10^{-2}	1.94× 10^{-10}	-7.05× 10^{-3}	1.53× 10^{-3}	5.66× 10^{-6}	-1.03× 10^{-2}	2.26× 10^{-3}	7.69× 10^{-6}
cg02782634	**17**	**57916643**	*VMP1*	7.80× 10^{-3}	1.20× 10^{-3}	2.41× 10^{-10}	-0.00865	1.64× 10^{-3}	2.16× 10^{-7}	-6.72× 10^{-3}	1.88× 10^{-3}	4.08× 10^{-4}
cg01079652	**1**	**79118191**	*IFI44*	-1.88× 10^{-2}	3.00× 10^{-3}	2.52× 10^{-10}	-01.88× 10^{-2}	4.00× 10^{-3}	3.76× 10^{-6}	-1.87× 10^{-2}	4.42× 10^{-3}	2.96× 10^{-5}
cg05883128	**4**	**169239131**	*DDX60*	-1.66× 10^{-2}	2.60× 10^{-3}	2.53× 10^{-10}	-1.37× 10^{-2}	3.29× 10^{-3}	4.67× 10^{-5}	-2.17× 10^{-2}	4.32× 10^{-3}	8.29 × 10^{-7}
cg05432003	**11**	**312518**	*IFITM1*	-1.05× 10^{-2}	1.70× 10^{-3}	2.66× 10^{-10}	-8.50× 10^{-3}	2.16× 10^{-3}	9.67× 10^{-5}	-1.33× 10^{-2}	2.59× 10^{-3}	4.86× 10^{-7}
cg05552874	**10**	**91153143**	*IFIT1*	-1.66× 10^{-2}	2.60× 10^{-3}	2.96× 10^{-10}	-1.38× 10^{-2}	3.40× 10^{-3}	6.27× 10^{-5}	-2.08× 10^{-2}	4.15× 10^{-3}	9.56× 10^{-7}
cg14392283	**8**	**144103587**	*LY6E*	-1.24× 10^{-2}	2.00× 10^{-3}	3.11× 10^{-10}	-1.17× 10^{-2}	2.52× 10^{-3}	4.93× 10^{-6}	-1.35× 10^{-2}	3.16× 10^{-3}	2.50× 10^{-5}
cg14750551	**3**	**122401343**	*PARP14*	-8.10× 10^{-3}	1.30× 10^{-3}	3.19× 10^{-10}	-0.00824	1.62× 10^{-3}	6.03× 10^{-7}	-7.80× 10^{-3}	2.10× 10^{-3}	2.43× 10^{-4}
cg00598235	**4**	**17580680**	*LAP3*	-5.80× 10^{-3}	9.00× 10^{-4}	4.67× 10^{-10}	-5.42× 10^{-3}	1.14× 10^{-3}	2.87× 10^{-6}	-6.51× 10^{-3}	1.60× 10^{-3}	6.06× 10^{-5}
cg26709300	**16**	**30106682**	*YPEL3*	5.80× 10^{-3}	9.0× 10^{-4}	5.41× 10^{-10}	5.34× 10^{-3}	1.23× 10^{-3}	1.78× 10^{-5}	6.35× 10^{-3}	1.42× 10^{-3}	1.15× 10^{-5}
cg18181703	**17**	**76354621**	*SOCS3*	-7.80× 10^{-3}	1.30× 10^{-3}	6.12× 10^{-10}	-8.27× 10^{-3}	1.66× 10^{-3}	9.85× 10^{-7}	-7.22× 10^{-3}	1.95× 10^{-3}	2.61× 10^{-4}
cg17114584	**11**	**613792**	*IRF7*	-1.17× 10^{-2}	1.90× 10^{-3}	6.51× 10^{-10}	-1.22× 10^{-2}	2.49× 10^{-3}	1.41× 10^{-6}	-1.11× 10^{-2}	2.95× 10^{-3}	2.00× 10^{-4}
cg01190666	**20**	**62204908**	*HELZ2*	-8.10× 10^{-3}	0.0013	6.87× 10^{-10}	-7.04× 10^{-3}	1.77× 10^{-3}	8.45× 10^{-5}	-0.00951	0.00198	2.36× 10^{-6}
cg01028142	**2**	**7004578**	*CMPK2*	-1.59× 10^{-2}	0.0026	8.89× 10^{-10}	-1.14× 10^{-2}	3.32× 10^{-3}	3.00× 10^{-5}	-1.91× 10^{-2}	4.20× 10^{-3}	8.00× 10^{-6}
cg17825130	**4**	**82283507**	*NA*	5.10× 10^{-3}	8.0× 10^{-4}	9.24× 10^{-10}	6.43× 10^{-3}	9.94× 10^{-4}	3.18× 10^{-10}	1.97× 10^{-3}	1.51× 10^{-3}	0.191
cg26312951	**21**	**42797847**	*MX1*	-1.61× 10^{-2}	2.60× 10^{-3}	9.91× 10^{-10}	-1.47× 10^{-2}	3.99× 10^{-3}	2.63× 10^{-4}	-1.73× 10^{-2}	3.53× 10^{-3}	1.56× 10^{-6}
cg21549285	**21**	**42799141**	*MX1*	-2.78× 10^{-2}	4.60× 10^{-3}	1.22× 10^{-9}	-2.25× 10^{-2}	6.18× 10^{-3}	3.18× 10^{-4}	-3.44× 10^{-2}	6.83× 10^{-3}	8.23× 10^{-7}
cg06473288	**6**	**32820102**	*TAP1*	-4.40 × 10^{-3}	7.0× 10^{-4}	1.24× 10^{-9}	-4.34 × 10^{-3}	8.49× 10^{-4}	5.04× 10^{-7}	-4.58× 10^{-3}	1.40× 10^{-3}	1.20 × 10^{--3}
cg06188083	**10**	**91093005**	*IFIT3*	-1.70× 10^{-2}	2.80× 10^{-3}	1.30× 10^{-9}	-1.60× 10^{-2}	3.75× 10^{-3}	2.65× 10^{-5}	-1.83× 10^{-2}	4.22× 10^{-3}	1.98× 10^{-5}
cg24898914	**6**	**32810706**	*PSMB8-AS1*	-4.30× 10^{-3}	7.00× 10^{-4}	1.30× 10^{-9}	-4.01× 10^{-3}	8.79× 10^{-4}	6.77× 10^{-6}	-5.00× 10^{-3}	1.24× 10^{-3}	6.95× 10^{-5}
cg16363586	**19**	**17516329**	*BST2; MVB12A; BISPR*	-6.10× 10^{-3}	1.00× 10^{-3}	1.90× 10^{-9}	-9.60× 10^{-3}	1.29× 10^{-3}	1.54× 10^{-7}	-4.83× 10^{-3}	1.67× 10^{-3}	4.12× 10^{-3}
cg13304609	**1**	**79085162**	*NA*	-1.59× 10^{-2}	2.60× 10^{-3}	1.94× 10^{-9}	-1.46× 10^{-2}	3.31× 10^{-3}	1.33× 10^{-5}	-1.81× 10^{-2}	4.39× 10^{-3}	4.93× 10^{-6}
cg03607951	**1**	**79085586**	*IFI44L*	-1.72× 10^{-3}	2.90× 10^{-3}	2.37× 10^{-9}	-1.56× 10^{-3}	3.87× 10^{-3}	6.94× 10^{-5}	-1.92× 10^{-2}	4.31× 10^{-3}	1.14× 10^{-5}

cg03110996	**2**	**191883483**	*NA*	-6.70× 10^{-3}	1.10× 10^{-3}	2.52× 10^{-10}	-5.36× 10^{-3}	1.38× 10^{-3}	1.30× 10^{-4}	-9.20× 10^{-3}	1.91× 10^{-3}	2.30× 10^{-6}
cg03084350	**3**	**38065265**	*PLCD1*	4.60× 10^{-3}	8.00× 10^{-4}	2.67× 10^{-9}	4.33× 10^{-3}	1.00× 10^{-3}	2.03× 10^{-5}	4.90× 10^{-3}	1.19× 10^{-3}	5.05× 10^{-5}
cg22488164	**12**	**14716910**	*PLBD1*	4.40× 10^{-3}	7.00× 10^{-4}	2.70× 10^{-9}	5.65× 10^{-3}	9.82× 10^{-4}	1.84× 10^{-8}	2.79× 10^{-3}	1.15× 10^{-3}	1.62× 10^{-2}
cg11694510	**11**	**313354**	*IFITM1*	-6.00× 10^{-3}	1.00× 10^{-3}	2.85× 10^{-9}	-5.79× 10^{-3}	1.28× 10^{-3}	9.28× 10^{-6}	-6.38× 10^{-3}	1.64× 10^{-3}	1.22× 10^{-4}
cg10778971	**14**	**94577101**	*IFI27*	-6.80× 10^{-3}	1.20× 10^{-3}	3.20× 10^{-9}	-5.25× 10^{-3}	1.39× 10^{-3}	1.92× 10^{-4}	-1.02× 10^{-2}	2.04× 10^{-3}	1.01× 10^{-6}
cg24681499	**1**	**42706997**	*FOXJ3*	3.50× 10^{-3}	6.00× 10^{-4}	4.11× 10^{-9}	3.49× 10^{-3}	6.80× 10^{-4}	4.71× 10^{-7}	3.44× 10^{-3}	1.20× 10^{-3}	4.35× 10^{-3}
cg16736826	**1**	**41951512**	*EDN2*	-5.10× 10^{-3}	9.00× 10^{-4}	4.35× 10^{-9}	-9.96× 10^{-3}	1.22× 10^{-3}	2.24× 10^{-8}	-3.15× 10^{-3}	1.22× 10^{-3}	1.06× 10^{-2}
cg19459791	**15**	**65363022**	*NA*	4.30× 10^{-3}	7.00× 10^{-4}	4.73× 10^{-9}	3.87× 10^{-3}	8.91× 10^{-4}	1.834× 10^{-5}	5.26× 10^{-3}	1.31× 10^{-3}	7.04× 10^{-5}
cg26250129	**17**	**79239903**	*SLC38A10*	5.20× 10^{-3}	9.00× 10^{-4}	4.98× 10^{-9}	5.23× 10^{-3}	1.10× 10^{-3}	3.17× 10^{-6}	5.17× 10^{-3}	1.50× 10^{-3}	6.74× 10^{-4}
cg16324306	**14**	**93786330**	*BTBD7*	6.30× 10^{-3}	1.10× 10^{-3}	5.92× 10^{-9}	6.65× 10^{-3}	1.29× 10^{-3}	3.97× 10^{-9}	5.42× 10^{-3}	1.99× 10^{-3}	6.69× 10^{-3}
cg05309505	**11**	**612837**	*IRF7*	-1.90× 10^{-3}	3.00× 10^{-4}	6.45× 10^{-9}	-1.71× 10^{-3}	4.12× 10^{-4}	4.41× 10^{-5}	-2.23× 10^{-3}	5.58× 10^{-4}	3.93× 10^{-5}
cg23892836	**6**	**29692085**	*HLA-F*	-7.10× 10^{-3}	1.20× 10^{-3}	8.43× 10^{-9}	-6.73× 10^{-3}	1.67× 10^{-3}	6.55× 10^{-5}	-7.44× 10^{-3}	1.81× 10^{-3}	4.92× 10^{-5}
cg01381586	**2**	**10587627**	*SNORA80B; ODC1*	-7.70× 10^{-3}	1.30× 10^{-3}	9.62× 10^{-9}	-7.88× 10^{-3}	1.85× 10^{-3}	2.61× 10^{-5}	-7.49× 10^{-3}	1.95× 10^{-3}	1.45× 10^{-4}
cg24925163	**2**	**128458248**	*SFT2D3*	3.40× 10^{-3}	6.00× 10^{-4}	9.67× 10^{-9}	3.75× 10^{-3}	6.75× 10^{-4}	5.9× 10^{-8}	2.26× 10^{-3}	1.30× 10^{-3}	8.30× 10^{-2}
cg00813162	**14**	**69443362**	*ACTN1*	3.60× 10^{-3}	6.00× 10^{-4}	1.07× 10^{-6}	3.05× 10^{-3}	8.41× 10^{-4}	3.88× 10^{-5}	3.83× 10^{-3}	9.76× 10^{-4}	1.05× 10^{-4}
cg05799596	**13**	**114909333**	*NA*	4.80× 10^{-3}	8.00× 10^{-4}	1.07× 10^{-8}	5.76× 10^{-3}	1.11× 10^{-3}	3.65× 10^{-7}	3.57× 10^{-3}	1.30× 10^{-3}	6.54× 10^{-3}
cg11393173	**1**	**116369577**	*NA*	-5.00× 10^{-3}	9.00× 10^{-4}	1.07× 10^{-8}	-5.41× 10^{-3}	1.07× 10^{-3}	7.49× 10^{-7}	-4.24× 10^{-3}	1.52× 10^{-3}	5.74× 10^{-3}
cg01721555	**3**	**122401300**	*PARP14*	-6.00× 10^{-3}	1.00× 10^{-3}	1.08× 10^{-8}	-5.63× 10^{-3}	1.27× 10^{-3}	1.27× 10^{-5}	-6.74× 10^{-3}	1.84× 10^{-3}	3.01× 10^{-4}
cg02297838	**13**	**92002454**	*MIR17HG; MIR17; MIR18A; MIR19A; MIR20A; MIR19B1; MIR92A1*	-6.70× 10^{-3}	1.20× 10^{-3}	1.11× 10^{-8}	-6.55× 10^{-3}	1.41× 10^{-3}	4.45× 10^{-6}	-7.01× 10^{-3}	2.12× 10^{-3}	1.04× 10^{-3}
cg15331332	**6**	**29692111**	*HLA-F*	-7.00× 10^{-3}	1.20× 10^{-3}	1.13× 10^{-8}	-6.44× 10^{-3}	1.53× 10^{-3}	3.32× 10^{-5}	-8.03× 10^{-3}	2.05× 10^{-3}	1.11× 10^{-4}
cg24002003	**15**	**101668143**	*NA*	-6.70× 10^{-3}	1.20× 10^{-3}	1.4× 10^{-8}	-6.94× 10^{-3}	1.55× 10^{-3}	1.023× 10^{-5}	-6.38× 10^{-3}	1.81× 10^{-3}	4.78× 10^{-4}
cg05622438	**3**	**51419127**	*DOCK3*	4.10× 10^{-3}	7.00× 10^{-4}	1.35× 10^{-8}	4.35× 10^{-3}	8.82× 10^{-4}	1.26× 10^{-6}	3.51× 10^{-3}	1.22× 10^{-3}	4.30× 10^{-3}
cg05696877	**1**	**79088769**	*IFI44L*	-2.39× 10^{-2}	4.20× 10^{-3}	1.47× 10^{-8}	-2.20× 10^{-2}	5.49× 10^{-3}	7.36× 10^{-5}	-2.65× 10^{-2}	6.66× 10^{-3}	6.934× 10^{-4}
cg02247863	**22**	**50983415**	*NA*	-5.40× 10^{-3}	1.00× 10^{-3}	1.50× 10^{-8}	-4.90× 10^{-3}	1.21× 10^{-3}	6.27× 10^{-5}	-6.21× 10^{-5}	1.55× 10^{-3}	7.51× 10^{-5}

cg09130674	**6**	**39195019**	*KCNK5*	-5.60× 10^{-3}	1.00× 10^{-3}	1.501× 10^{-8}	-5.20× 10^{-3}	1.36× 10^{-3}	1.64× 10^{-4}	-6.09× 10^{-3}	1.45× 10^{-3}	3.31× 10^{-5}
cg20408505	**6**	**29911494**	*HLA-A*	-8.10× 10^{-3}	1.40× 10^{-3}	1.88× 10^{-7}	-7.21× 10^{-3}	1.91× 10^{-3}	1.82× 10^{-4}	-9.28× 10^{-3}	2.20× 10^{-3}	3.17× 10^{-5}
cg27333269	**1**	**15739283**	*EFHD2*	3.70× 10^{-3}	7.00× 10^{-4}	2.06× 10^{-8}	3.26× 10^{-3}	7.58× 10^{-4}	2.19× 10^{-5}	5.03× 10^{-3}	1.33× 10^{-3}	1.88× 10^{-4}
cg11187245	**6**	**31323397**	*HLA-B;MIR6891*	-7.60× 10^{-3}	1.40× 10^{-3}	2.07× 10^{-8}	-7.37× 10^{-3}	1.76× 10^{-3}	3.44× 10^{-5}	-7.89× 10^{-3}	2.12× 10^{-3}	2.32× 10^{-4}
cg17052170	**8**	**144099482**	*LY6E;LOC100133669*	-1.55× 10^{-2}	2.80× 10^{-3}	2.12× 10^{-8}	-1.39× 10^{-2}	4.13× 10^{-3}	8.13× 10^{-4}	-1.68× 10^{-2}	3.74× 10^{-3}	9.57× 10^{-6}
cg13007871	**6**	**30458519**	*HLA-E*	-7.20× 10^{-3}	1.30× 10^{-3}	2.23× 10^{-8}	-6.22× 10^{-3}	1.64× 10^{-3}	1.77× 10^{-4}	-8.85× 10^{-3}	2.09× 10^{-3}	3.03× 10^{-5}
cg01281718	**6**	**71376634**	*SMAP1*	4.10× 10^{-3}	7.00× 10^{-4}	2.26× 10^{-8}	5.14× 10^{-3}	8.57× 10^{-4}	4.87× 10^{-9}	1.32× 10^{-3}	1.36× 10^{-3}	0.332
cg12686273	**16**	**3085867**	*LOC100128770;CCDC64B*	-6.40× 10^{-3}	1.20× 10^{-3}	2.67× 10^{-8}	-6.56× 10^{-3}	1.50× 10^{-3}	1.57× 10^{-6}	-6.24× 10^{-3}	1.82× 10^{-3}	6.78× 10^{-4}
cg00490406	**1**	**159046773**	*AIM2*	-1.11× 10^{-2}	2.00× 10^{-3}	2.68× 10^{-8}	-1.35× 10^{-2}	2.62× 10^{-3}	7.655× 10^{-7}	-8.10× 10^{-3}	2.97× 10^{-3}	6.80× 10^{-3}
cg00546932	**16**	**1947055**	*NA*	-3.90× 10^{-3}	7.00× 10^{-4}	2.76× 10^{-8}	-5.17× 10^{-3}	9.79× 10^{-4}	2.21× 10^{-7}	-2.56× 10^{-3}	1.01× 10^{-3}	1.18× 10^{-2}
cg11702942	**8**	**144102584**	*LY6E*	-7.00× 10^{-3}	1.30× 10^{-3}	2.81× 10^{-8}	-6.28× 10^{-3}	1.56× 10^{-3}	1.64× 10^{-5}	-7.50× 10^{-3}	2.18× 10^{-3}	6.63× 10^{-4}
cg26987613	**6**	**33219410**	*HCG25; VPS52*	-4.30× 10^{-3}	8.00× 10^{-4}	2.94× 10^{-9}	-4.06× 10^{-3}	8.97× 10^{-8}	8.32× 10^{-6}	-5.20× 10^{-3}	1.59× 10^{-3}	1.19× 10^{-3}
cg02650017	**17**	**47301614**	*PHOSPHO1*	-3.70× 10^{-3}	7.09× 10^{-4}	3.00× 10^{-8}	-3.95× 10^{-3}	8.32× 10^{-4}	2.98× 10^{-6}	-3.32× 10^{-3}	1.15× 10^{-3}	4.11× 3
cg23580000	16	**50322156**	*ADCY7*	5.70× 10^{-3}	1.01× 10^{-3}	3.16× 10^{-8}	6.75× 10^{-3}	1.31× 10^{-3}	4.30× 10^{-7}	3.96× 10^{-3}	1.63× 10^{-3}	1.56× 10^{-2}
cg08926253	**11**	**614761**	*IRF7*	-1.04× 10^{-2}	1.92× 10^{-3}	3.32× 10^{-8}	-9.21× 10^{-3}	2.38× 10^{-3}	1.31× 10^{-4}	-1.22× 10^{-2}	3.03× 10^{-3}	7.26× 10^{-}5
cg18533225	**22**	**50986813**	*KLHDC7B*	-1.01× 10^{-2}	1.84× 10^{-3}	3.31× 10^{-8}	-8.96× 10^{-3}	2.64× 10^{-3}	7.76× 10^{-4}	-1.11× 10^{-2}	2.53× 10^{-3}	1.48× 10^{-5}
cg25800166	**12**	**113375896**	*OAS3*	-7.80× 10^{-3}	1.40× 10^{-3}	3.49× 10^{-9}	-6.01× 10^{-3}	1.79× 10^{-3}	8.96× 10^{-4}	-1.06× 10^{-2}	2.23× 10^{-3}	4.64× 10^{-6}
cg03590328	**7**	**2684462**	*TTYH3*	4.00× 10^{-3}	7.0× 10^{-4}7	3.98× 10^{-8}	5.12× 10^{-3}	9.60× 10^{-4}	1.68× 10^{-7}	2.50× 10^{-3}	1.14× 10^{-3}	2.96× 10^{-2}
cg07461273	**7**	**99697172**	*MCM7*	3.80× 10^{-3}	7.01× 10^{-4}	4.11× 10^{-8}	3.51× 10^{-3}	8.58× 10^{-4}	5.25× 10^{-5}	4.17× 10^{-3}	1.13× 10^{-3}	2.76× 10^{-4}
cg26234900	**6**	**32820214**	*TAP1*	-3.80× 10^{-3}	7.00× 10^{-4}	4.20× 10^{-9}	-4.24× 10^{-3}	8.22× 10^{-4}	4.25× 10^{-7}	-2.71× 10^{-3}	1.27× 10^{-3}	3.42× 10^{-2}
cg09304968	**7**	**76977748**	*GSAP*	2.20× 10^{-3}	4.02× 10^{-4}	4.22× 10^{-8}	2.05× 10^{-3}	4.49× 10^{-5}	7.03× 10^{-6}	3.21× 10^{-3}	9.96× 10^{-4}	1.39× 10^{-3}
cg03963853	**16**	**4732369**	*MGRN1*	5.10× 10^{-3}	9.08× 10^{-4}	4.34× 10^{-8}	5.16× 10^{-3}	1.08× 10^{-3}	2.76× 10^{-6}	4.96× 10^{-3}	1.83× 10^{-3}	7.14× 10^{-3}
cg03149958	**6**	**36326677**	*ETV7*	-5.50× 10^{-3}	1.03× 10^{-3}	4.86× 10^{-8}	-4.55× 10^{-3}	1.27× 10^{-3}	3.83× 10^{-4}	-7.12× 10^{-3}	1.66× 10^{-3}	2.33× 10^{-5}
cg26227957	**1**	**19547285**	*EMC1*	4.70× 10^{-3}	9.03× 10^{-4}	5.05× 10^{-8}	5.62× 10^{-3}	1.09× 10^{-3}	3.85× 10^{-7}	3.14× 10^{-3}	1.42× 10^{-3}	2.77× 10^{-2}
cg22505006	**1**	**154981829**	*ZBTB7B*	4.20× 10^{-3}	8.05× 10^{-4}	6.23× 10^{-8}	4.94× 10^{-3}	9.61× 10^{-4}	4.54× 10^{-7}	2.79× 10^{-3}	1.29× 10^{-3}	3.09× 10^{-2}

cg00007076	**8**	**67342600**	*RRS1-AS1*	-7.10× 10^{-3}	1.35× 10^{-3}	6.33× 10^{-8}	-7.31× 10^{-3}	1.58× 10^{-3}	5.31× 10^{-6}	-6.51× 10^{-3}	2.30× 10^{-3}	5.00× 10^{-3}
cg14864167	**8**	**66751182**	*PDE7A*	-1.82× 10^{-2}	3.44× 10^{-3}	7.02× 10^{-8}	-1.84× 10^{-3}	4.41× 10^{-3}	3.85× 10^{-5}	-1.80× 10^{-2}	5.27× 10^{-3}	7.00× 10^{-4}
cg16411857	**16**	**57023191**	*NA*	-7.60× 10^{-3}	1.47× 10^{-3}	7.77× 10^{-8}	-6.46× 10^{-3}	1.98× 10^{-3}	1.24× 10^{-3}	-8.66× 10^{-3}	1.99× 10^{-3}	1.87× 10^{-5}
cg01153613	**6**	**139928856**	*NA*	4.30× 10^{-3}	8.01× 10^{-4}	8.02× 10^{-8}	5.43× 10^{-3}	9.82× 10^{-3}	6.24× 10^{-8}	2.05× 10^{-3}	1.40× 10^{-3}	0.143
cg12854186	**6**	**32805398**	*TAP2*	-6.30× 10^{-3}	1.20× 10^{-3}	8.52× 10^{-8}	-5.08× 10^{-3}	1.50× 10^{-3}	7.82× 10^{-4}	-8.16× 10^{-3}	1.88× 10^{-3}	1.91× 10^{-5}
cg25630380	**1**	**156784869**	*NTRK1; SH2D2A*	-3.20× 10^{-3}	6.09× 10^{-4}	9.45× 10^{-8}	-4.00× 10^{-3}	7.91× 10^{-4}	6.85× 10^{-7}	-2.14× 10^{-3}	9.37× 10^{-4}	2.28× 10^{-2}
cg11791770	**11**	**611791**	*PHRF1*	-3.90× 10^{-3}	7.02× 10^{-4}	9.56× 10^{-8}	-3.49× 10^{-3}	9.01× 10^{-4}	1.27× 10^{-4}	-4.85× 10^{-3}	1.29× 10^{-3}	1.97× 10^{-4}
cg18006990	**6**	**43594962**	*GTPBP2*	-3.40× 10^{-3}	6.05× 10^{-4}	1.03× 10^{-7}	-3.84× 10^{-3}	8.28× 10^{-4}	4.96× 10^{-6}	-2.70× 10^{-3}	9.78× 10^{-4}	6.07× 10^{-3}
cg00417304	**11**	**45124456**	*PRDM11*	-5.10× 10^{-3}	1.06× 10^{-3}	1.02× 10^{-7}	-5.90× 10^{-3}	0.1.19× 10^{-3}	1.01× 10^{-6}	-3.57× 10^{-3}	1.62× 10^{-3}	2.80× 10^{-2}
cg26077811	**11**	**119232263**	*USP2*	-4.90× 10^{-3}	9.00× 10^{-4}	1.10× 10^{-7}	-5.50× 10^{-3}	1.20× 10^{-3}	6.27× 10^{-6}	-4.07× 10^{-3}	1.46× 10^{-3}	5.67× 10^{-3}
cg11601443	**12**	**113415930**	*OAS2*	-3.90× 10^{-3}	7.00× 10^{-4}	1.10× 10^{-7}	-3.17× 10^{-3}	9.07× 10^{-4}	5.37× 10^{-4}	-5.13× 10^{-3}	1.22× 10^{-3}	3.5× 10^{-5}
cg15844711	**11**	**59435407**	*PATL1*	-5.90× 10^{-3}	1.12× 10^{-3}	1.11× 10^{-7}	-5.50× 10^{-3}	1.30× 10^{-3}	2.94× 10^{-5}	-6.88× 10^{-3}	2.12× 10^{-3}	1.32× 10^{-3}
cg18125510	**14**	**100841768**	*WARS; WDR25*	-6.30× 10^{-3}	1.25× 10^{-3}	1.23× 10^{-7}	-6.39× 10^{-3}	1.56× 10^{-3}	5.12× 10^{-5}	-6.22× 10^{-3}	1.86× 10^{-3}	9.11× 10^{-4}
cg0612808	**2**	**113404678**	*SLC20A1*	-6.00× 10^{-3}	1.81× 10^{-3}	1.25× 10^{-7}	-5.37× 10^{-3}	1.51× 10^{-3}	4.10× 10^{-4}	-6.82× 10^{-3}	1.73× 10^{-3}	9.60× 10^{-5}
cg08289839	**13**	**111318640**	*CARS2*	4.00× 10^{-3}	8.90× 10^{-4}	1.32× 10^{-7}	4.66× 10^{-3}	9.45× 10^{-4}	1.26× 10^{-6}	2.81× 10^{-3}	1.26× 10^{-3}	2.68×10^{-2}

SE: standard error of beta coefficient; NA: not available.

Supplementary Table 3. Summary of Significant CpG sites in EPIC chip, but Not replicable 450K chip

CpG Site	Chr	Beta	P-value in EPIC subset	Annotated Gene name	Bonferroni P-value	Fdr q-value
cg05475649	15	-0.0222	5.32×10^{-10}	B2M	0.000450	0.000264
cg12828896	15	-0.0265	8.15×10^{-10}	B2M	0.000690	0.000264
cg27537252	15	-0.0256	9.89×10^{-10}	B2M	0.000837	0.000264
cg07815522	3	-0.0323	1.25×10^{-9}	PARP9; DTX3L	0.00106	0.000264
cg01082299	6	-0.0171	7.31×10^{-9}	HCP5	0.00619	0.000669
cg03425812	15	-0.0255	7.91×10^{-9}	B2M	0.00669	0.000669
cg21979287	15	-0.0151	9.35×10^{-9}	B2M	0.00792	0.000792
cg00272009	3	-0.0170	1.33×10^{-8}	PARP14	0.0113	0.000939
cg08888522	2	-0.0182	5.10×10^{-8}	IFIH1	0.0432	0.00225
cg06716655	1	-0.0145	5.31×10^{-8}	ADAR	0.0449	0.00225
cg18387107	12	-0.0142	5.79×10^{-8}	PARP11	0.0490	0.00233
cg04880620	12	-0.00983	6.53×10^{-8}	OAS2	0.0452	0.00240